Chapter 5
Biological Tissue Imaging at Different Levels: MALDI and SIMS Imaging Combined

J. Stauber and Ron M.A. Heeren

Abstract Mass spectrometry has been employed to analyze the composition and structure of biologically relevant molecules in solution. Advances in methodology and instrumentation developments now allow the application of mass spectrometry for local biomolecular analysis directly on biological tissue surfaces; this technique is called imaging mass spectrometry (IMS). IMS is an innovative discovery tool for the biomedical sciences. This chapter describes the two main approaches relevant for molecular tissue imaging studies in the life sciences: secondary ion mass spectrometry (SIMS) imaging and matrix-assisted laser desorption and ionization (MALDI)–based imaging techniques. The benefits of imaging mass spectrometry for the fields of drug metabolism, lipidomics, and proteomics are discussed. Integrated MS imaging and proteomics protocols as well as tandem-MS imaging strategies, which are key to the identification of larger-molecular-weight compounds, are also reviewed.

5.1 Introduction

Imaging mass spectrometry (IMS) [1] is a very sensitive molecular imaging technique that provides combined molecular resolution and spatial resolution. It allows the identification and localization of the molecular content directly from tissue sections, single cells, and many other surfaces. The key features for biological studies are the sensitivity provided by modern mass spectrometers, the label-free nature of the technique, the ability to image posttranslational modifications, and the spatial resolution, which ranges from the organisms level (hundreds of micrometers) to the

J. Stauber • R.M.A. Heeren (✉)

FOM-Institute for Atomic and Molecular Physics, Science park 104,
1098 XG Amsterdam, The Netherlands
e-mail: heeren@amolf.nl
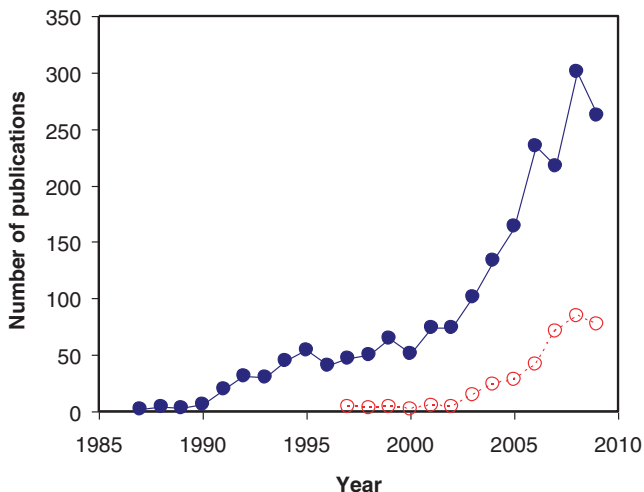
Fig. 5.1 The number of publications resulting from a "web-of-science" search using the keywords "MALDI imaging" (*open circles*) and "imaging mass spectrometry" (*solid circles*). The results were obtained from the December 31, 2009, database

cellular level (tens of nanometers). IMS allows the simultaneous detection and imaging of thousands of species images in a single experiment. As such, it constitutes an efficient, multicomponent molecular imaging technique. The large number of new studies that include imaging mass spectrometry is evidence of the rapid growth of the field (Fig. 5.1).

IMS can be used to study different compositions and structures of surfaces in the context of biological studies. The IMS protocols and instruments have been developed to study the biodistribution of endogenous compounds, such as lipids or proteins, and exogenous compounds, such as polymers or drugs designed for tissue treatment. IMS helps to understand biological processes from subcellular to multicellular levels of spatial resolution. Moreover, it detects many different types of compounds in order to cover the large number of molecules present in the animal and vegetable kingdoms.

Compared to other molecular imaging approaches, such as magnetic resonance imaging (MRI), positron emission tomography (PET), or fluorescent immunochemistry, IMS provides unique information: IMS identifies molecules without the labeling of compounds, which allows the discovery of new localized compounds; no other technique can do this. Even though IMS is an Ex vivo technique and not an in vivo diagnosis technique such as MRI or PET, it can be coupled with them to validate molecular repartition, examine degradation of biomarkers, and/or study drug delivery, as demonstrated in recent publications [2].

Biological surface analysis with mass spectrometry has evolved around two main desorption and ionization methods: secondary ion mass spectrometry (SIMS) and matrix-assisted laser desorption ionization (MALDI). Both techniques are used

in imaging mass spectrometry and combined with different mass analyzers and detectors in order to increase the sensitivity and spatial resolution. SIMS has been in development since the early 1970s and applied to many different biological surfaces [2]. Although SIMS was initially limited to elements and small molecules, the detection and imaging of higher-molecular-weight species were realized through different surface modifications, such as metal-assisted SIMS (MetA-SIMS) and matrix-enhanced SIMS (ME-SIMS) [3–5], as well as by the use of cluster ion beam as the projectile species, as outlined in Chap. 4 of this book. MALDI imaging was developed in the late 1990s to image larger, intact molecules such as peptides and proteins. The SIMS and MALDI techniques both possess complementary characteristics in mass range, sensitivity, and spatial resolution, as will be demonstrated in this chapter.

IMS is crucially dependent on suitable and adequate sample-preparation techniques, as is any molecular analytical technique. Sample preparations, including solvent treatment, sample storage, and matrix deposition, are important for classical proteomics and lipidomics experiments directly on tissue. Reproducible sample preparations allow sensitive and high-resolution image analysis with ME-SIMS, MetA-SIMS, and MALDI imaging. Due to the different sensitivities and mass ranges accessible by SIMS and MALDI, different classes of molecules can be detected by combining these techniques [6]. Peptides and proteins, as well as lipids, metals, drugs, and metabolites, can be monitored and localized in different biological samples. Combinations of specific (bio-)markers that characterize a disease state can be identified, as IMS provides simultaneous images of different compounds found on pathological tissue sections.

In this chapter, we present the three biomolecular IMS techniques (ME-SIMS, MetA-SIMS, and MALDI), discuss different tissue-preparation methods, and summarize representative applications in different fields of research, such as lipidomics, plant studies, pharmaceuticals, proteomics, and clinical proteomics. The chapter ends with an outlook on future developments and the related applications of surface-enhanced SIMS and MALDI imaging. These high-end mass-spectrometric–based imaging methodologies are continuously under development to improve the sensitivity, resolution (both spatial and mass-resolving power), and data workup protocol, in order to increase the usage of IMS in clinical medicine.

5.2   Imaging Mass Spectrometry Modes

5.2.1   Imaging Modes

Many different ionization methods and mass analyzers have been used in imaging mass spectrometry (IMS) experiments. SIMS and MALDI have emerged as the two dominant methodologies in the generation of mass-resolved molecular images of surfaces. Both display different but complementary molecular imaging capabilities

and are employed in a wide variety of (biological) applications. Traditionally, SIMS targeted elements and small to medium-sized biomolecules (under 600 Da), whereas MALDI extended molecular imaging capabilities to a larger-molecular-weight domain (100 Da–80 kDa).

The two techniques combine an ion source, a mass analyzer, an ion detector, and data acquisition and processing software. They display complementary spatial resolution, sensitivity, and molecular weight ranges. Two different types of imaging modes, irrespective of the ionization method, are used: microprobe mode imaging and microscope mode imaging. The next section briefly explains the two different imaging approaches

5.2.2   Microprobe Mode

Microprobe (Fig. 5.2) is the most common imaging mode in mass spectrometry. It is a relatively straightforward technique to image a small, localized region by focusing a desorption/ionization beam on the sample. The ionization beam rasters, or scans, a selected region of the sample, and a mass spectrum is recorded for each beam shot. The mass spectra are stored along with the coordinates of the analyzed spot, as defined by the focus and position of the ionization beam. Molecular images of different ions are retrospectively reconstructed by dedicated software. This microprobe scanning mode is usually used with SIMS and MALDI imaging mass spectrometry. The spatial resolution of the ionization beam can be as high as 50 nm in SIMS and is conventionally limited by the laser spot's size (typically 50 μm) in MALDI. For that reason, the microscope imaging mode was developed and applied for MALDI studies in order to increase the spatial resolution [7].

5.2.3   Microscope Mode

The microscope imaging (Fig. 5.2) mode does not require position rastering with focused desorption beams. Instead, ion-optical elements in the time-of-flight mass spectrometer are used to retain the spatial organization of the ions after desorption and ionization between the ion source and the detector [7]. This results in a mass-resolved projection of the spatial origin of the ions generated at the sample surface by the defocused ionization beam and allows direct mass-resolved molecular image observation when combined with a position-sensitive detector. The magnification of the microscope elements, the quality of the ion optics, and the resolution of the position-sensitive detector determine the spatial resolution. The best spatial resolution demonstrated to date is a pixel size of 600 nm [7, 8]. The microscope mode directly analyzes a larger field-of-view (FOV) than the microprobe mode: It allows for the analysis of up to a 400-μm-diameter area. The microscope mode is approximately 10,000 times faster than the microprobe mode.
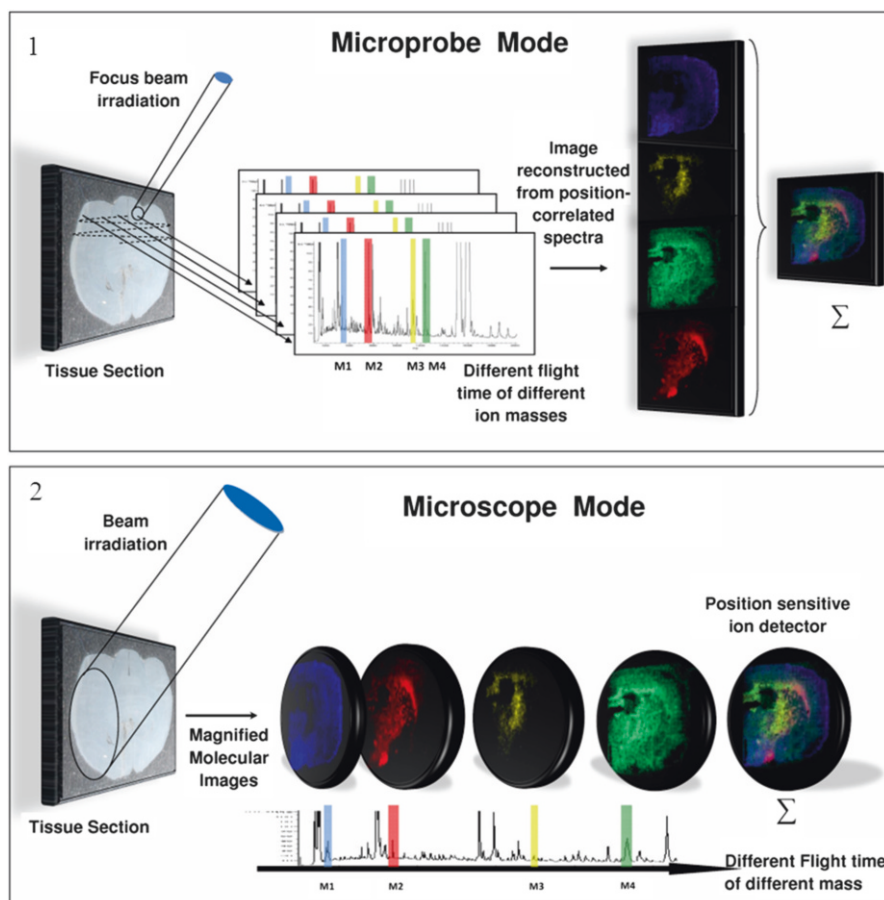
Fig. 5.2 Schematics illustrating the two approaches in molecular imaging mass spectrometry: (**1**) Microprobe-mode imaging records the mass spectra in spot-by-spot (x, y) position on the sample surface; (**2**) microscope-mode imaging records magnified images of mass-resolved ion distributions using a 2D detector

5.3 MALDI and SIMS: Two Sources of Ionization

5.3.1 MALDI Source

Developed by Karas and Hillenkamp in 1987 [9, 10], MALDI allows the simultaneous ionization/desorption of sample molecules, provides high sensitivity, and allows the analysis of large (up to 200 kDa) molecules. MALDI imaging was introduced in 1997 with advanced software capabilities [11, 12]. A large number of applications were presented in the last decade, with many biological applications. Most studies

use the MALDI imaging technique in a microprobe mode, by combining laser irradiation of the sample and advanced software capabilities to reconstruct images. More recently, commercial instruments with well-optimized system control and a laser spot size down to approximately a 50-μm diameter have been developed. Important MALDI considerations include the size of the laser beam, the wavelength, the pulse width, and the matrices used. MALDI imaging traditionally uses either N2 (337-nm) or Nd:YAG (335-nm) UV lasers, with the latter becoming more routinely used over the last two years, resulting in increased laser performance and stability. The laser pulse length (width) was found to have very little to no influence on MALDI mass spectra, at least up to pulse lengths of tens of nanoseconds [13]. This suggests that the desorption/ionization process is determined by the energy density supplied to the sample by the laser pulse (fluence or energy density, 100 J/m^2) rather than by the rate of energy flow (irradiance, W/cm^2). The fluence or energy flow required on the target is dependent on the spot size and pulse length (typically 3–5 ns).

(a) *Desorption/ionization process*

Since 1976, laser irradiation has been employed to ionize peptides from solid samples deposited on a surface [14]. Studies over the first decade of its use showed it was not efficient for large peptides. Therefore, the use of a matrix as an energy-transfer medium presented advantages in the desorption/ionization laser process.

The technique of MALDI imaging uses a pulsed beam of laser in the UV (or infrared laser source) to desorb and ionize a mixture of co-crystallized matrix and tissue. The matrix minimizes the sample degradation caused by energy absorption of the laser beam. The laser-transmitted energy is absorbed by the matrix, which acts as a resonant absorber for the photons and causes a phase explosion due to overheating of the surface. The sample molecules expand, are ejected into the gas phase, ionized, and then detected.

Partially ejected molecules are ionized by proton transfer, in the solid phase either before desorption or after desorption by collision with the excited matrix and other molecules. These processes generate different singly or multiply charged ions [M+nH]$^{n+}$, but the majority are singly charged ions.

No single mechanism can explain all the ions observed in a MALDI experiment. The large range of samples, matrices, and experimental parameters hinders the elucidation of ion-formation mechanisms. However, ion-formation mechanisms are described by two categories: primary and secondary ion formation [15]. The timescale for ion formation is of utmost interest, where the laser pulse typically lasts 3–5 ns, but the time required for expansion is much longer, many microseconds [16]. Primary ionization is caused by the laser pulse directly or by ion-molecule reactions within the excited matrix plume. Basic thermodynamics of ion formation, multiphoton ionization [17], energy pooling [18], and excited-state proton transfer [9] describe primary ionization. Although many primary ionization pathways have been identified, it has been hypothesized that secondary processes that occur within the expanding plume of sputtered species are the most important factor for the production of ions [19, 20]. In the expanding plume, reactions between ions and neutrals continue as long as there are collisions. Electron and proton transfer from the

matrix to the analyte is probably the most important secondary reaction and causes the predominantly detected protonated form of peptides and proteins. The gas-phase reaction of these two products is exoergic (protonation of peptide and deprotonation of matrix) since the proton affinity of the matrix is lower than the gas-phase basicity (GB) of the peptides or proteins, while the deprotonation of peptides and proteins is endoergic [20].

(b) *The matrix: The key role in a MALDI imaging experiment*

As explained above, the thermodynamics of the reaction depends on the type of matrix employed. Each matrix–analyte system exhibits different proton-transfer energetics. Therefore, different matrices are used for different types of analytes.

Figure 5.3 shows MALDI matrices and their structures. Three matrices are commonly used: 3,5-dimethoxy-4-hydroxycinnamic acid (sinapinic acid, SA), α-cyano-4-hydroxycinnamic acid (HCCA), and 2,5-dihydroxybenzoic acid (DHB). SA is specially used as a more energetic matrix for the detection of proteins between 2 and 75 kDa. However, SA generates many derived ions at a low mass range, which results in a large amount of chemical noise [20]. Thus, for peptide ion detection, HCCA or DHB is often used. These cold matrices do not generate as much derived ion signal at low mass and allow easy mass spectral analysis and image reconstructions..

Recently, ionic matrices have been applied [21], to improve the signal intensities and crystal size homogeneity. These ionic matrices are obtained by a reaction between an acid matrix and a base (aniline). The comparison of images between classical matrix and ionic matrix HCCA/ANI positions them as an alternative to classical matrices (Fig. 5.4).

5.3.2   SIMS Source

Secondary ion mass spectrometry has been used as a high-spatial-resolution analytical microscopy technique since its inception as an imaging technique. Developed by Castaing and Slozdian in 1962 [2], a broad beam (0.5-mm diameter of Ar^+ primary ion beam) was used to desorb and ionize sample in a secondary ion and create an image resulting in a 1-μm spatial resolution. In the microscope mode, the ultimate spatial resolution of mass-resolved images is comparable to that of the best optical microscopes (0.5 μm). This limitation is imposed by the energy spread of the secondary ions, causing imaging chromatic aberrations. The microprobe scanning mode, which was developed to be an alternative SIMS imaging mode [22], and the introduction of high-brightness liquid ion sources (LMIS) revolutionized SIMS imaging mass spectrometry in the 1980s. These ion sources, with suitable apertures and focusing ion optics, can be focused to small spot sizes (in the best case 20 nm) while retaining sufficient ion current for high-spatial-resolution microprobe experiments [23]. SIMS coupled with a time-of-Flight (ToF) analyzer provides a technique with high spatial resolution and high mass-resolving power and allows for the simultaneous detection of all species.
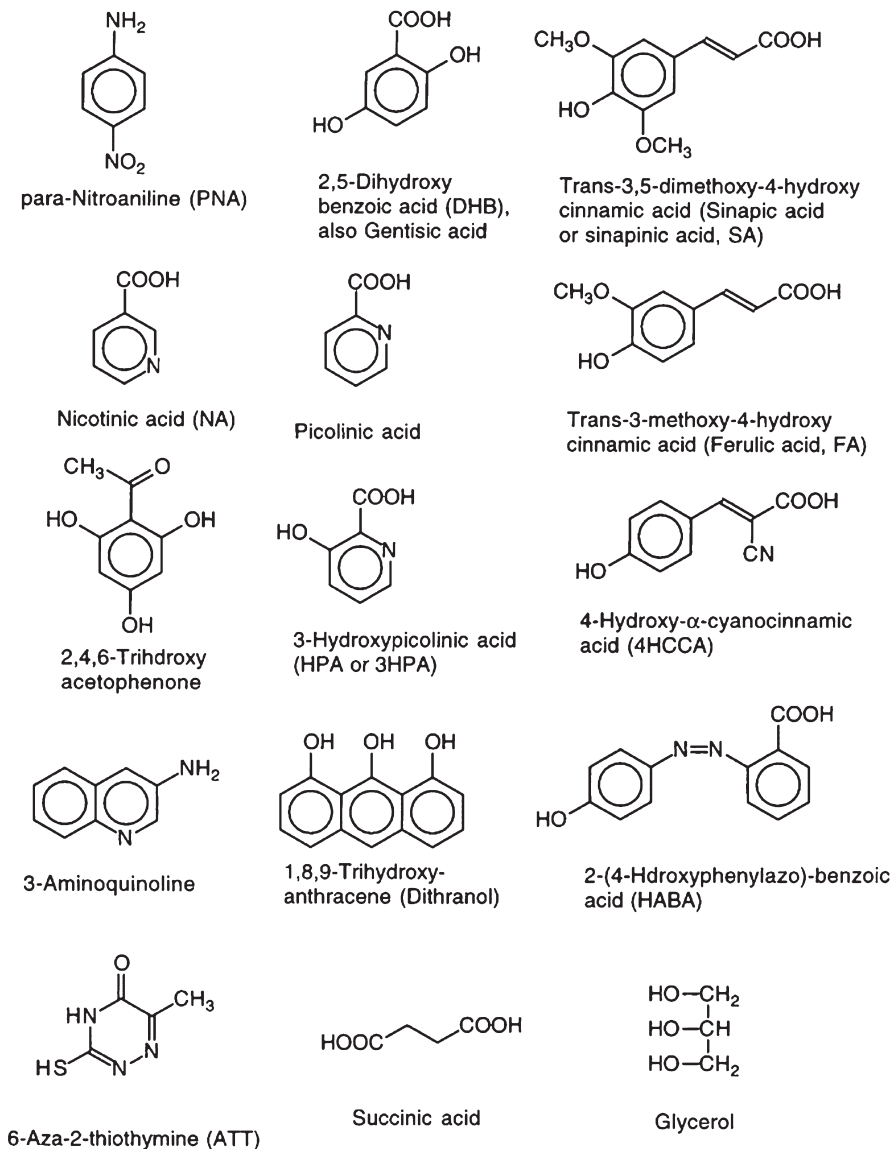
Fig. 5.3 Structures, chemical names, trivial names, and abbreviations of frequently used MALDI matrices (From Ref. [15])

(a) *Enhancing molecular ion yield in SIMS*

SIMS is one dominant technique for surface analysis and imaging by mass spectrometry of small molecules [24]. Here, we discuss strategies that can enhance the applicability of SIMS to biological tissue surfaces. These innovative strategies, which include matrix-enhanced SIMS and metal-assisted SIMS, complement the MALDI-based imaging approaches.
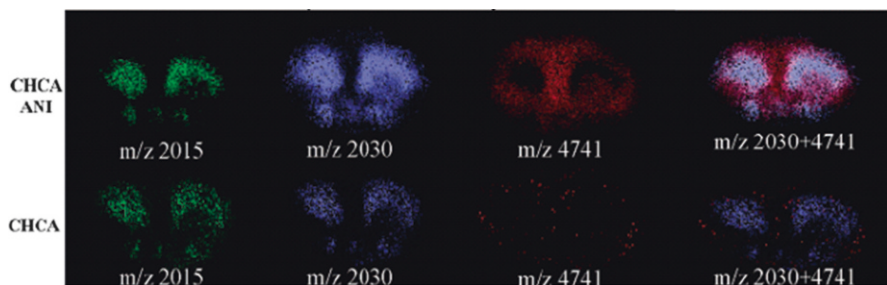
Fig. 5.4 Comparison of HCCA classical matrix (*bottom*) and HCCA/ANI ionic matrix (*top*). The HCCA/ANI matrix shows higher signal intensities than the classical HCCA matrix [21]

The sputtering process in SIMS, generated by high-energy primary ions, results in fragmentation of almost all labile components on the surface. Increased detection sensitivity for these labile intact molecular ions has been a major research topic in organic SIMS for more than 10 years. Several strategies have been developed to minimize the internal energy deposition during desorption and ionization in SIMS.

The use of polyatomic primary ion sources, such as C_{60}^+, SF_6^-, Au_n, and Bi_n^{m+}, results in an increased secondary ion yield [25, 26]. Here, a beam of energetic cluster ions (up to several thousand electron volts) is directed at the surface. The cluster ions are believed to dissociate at the moment of surface impact, which results in the redistribution of the initial kinetic energy over the atoms present in the cluster [26, 27]. ME-SIMS (matrix-enhanced SIMS [28]) and MetA-SIMS (metal-assisted SIMS [3, 29]) have also been developed to increase the dynamic mass range, as outlined below.

(b) *Matrix-enhanced SIMS*

Odom and Wu reported the first ME-SIMS results in 1996. In their study, the sample was prepared in a solid organic matrix similar to sample preparations used for MALDI [28]. Over the past decade, ME-SIMS has been applied to a variety of biological studies [3, 5, 30]. This technique requires specific sample-preparation steps in order to optimize the signal intensity and minimize the redistribution or modification of the sample analytes.

The idea of diluting analyte molecules in a solid matrix preceded the invention of MALDI. Michl and coworkers analyzed small organic molecules by SIMS with frozen rare gas (Ar) as a matrix [31]. Other groups investigated the use of carbon as a matrix, which is particularly helpful in the analysis of polycyclic aromatic compounds [32, 33]. Barber and coworkers also popularized the use of glycerol matrices for ME-SIMS. In comparison with solid matrices, the liquid matrix refreshes the sample by evaporation and/or macroscopic flow under ion beam bombardment conditions [34]. Gillen et al. reported enhanced secondary ion signals for small molecules embedded in frozen glycerol matrix [35] and also studied gelatin matrices as a model of biological samples for secondary ion emission [36]. In addition, Cooks and coworkers embedded samples in ammonium chloride [37]. Similarly, Wu and

Odom applied a solid organic matrix similar to sample preparations used in MALDI for high-mass detection [28]. The co-crystallization of the matrix on the sample surface permits the observation of molecular ions using static secondary ion mass spectrometry (SSIMS). Matrix-enhanced SIMS yields substantial increases in the ionization efficiency of peptides, proteins, and oligonucleotides, enabling the detection of species with masses up to ~10,000 Da.

5.3.3   Characteristic of Ionization, Differences Between SIMS and Matrix-Enhanced SIMS

Cooks and coworkers report that the use of a matrix such as NH_4Cl results in the ejection of ions with a lower internal energy since fewer fragmentation products are observed in the mass spectra [37, 38]. The authors proposed that analyte and matrix molecules are sputtered from the surface in the form of clusters. After emission, these clusters cool via evaporation, releasing analyte molecules with a low internal energy.

Other authors [28, 39] have compared a series of MALDI matrices and biological analytes with various masses (MW: 1,759–14,000 Da) in order to assess positive/negative matrix and the ion analyte yields. It is not clear what proportion of the efficiency enhancement provided by the matrix is attributable to the dynamics of desorption and to the chemistry of the molecular ion-emission ionization steps. It is proposed that the matrix plays an essential role as a strong proton donor, such as those used as MALDI matrices [37]. In the ME-SIMS process, the matrix should efficiently promote the cationization of neutral molecules sputtered from a solid mixture by an energetic ion beam, without photochemical reactions initiated by UV laser photons. In addition, a large number of molecules are sputtered per ion impact, and the analyte appears to be naturally entrained by the sputtered matrix flux. Moreover, the use of a matrix/analyte mixture yields less fragmentation, which is attributed to the excess matrix in the environment, which provides a much softer yet efficient desorption and ionization of the compound [28]. Finally, the matrix/analyte mixture has a sufficiently high concentration of analytes in the top monolayers of the surface.

5.3.4   Characteristic of Metal-Assisted SIMS

Surface metallization (MetA-SIMS) was also developed to enhance the desorption/ionization of higher-molecular-mass species [40]. For MetA-SIMS, a submonolayer coverage of a noble metal such as Au or Ag is applied to the surface of a material. Silver and gold metallization demonstrated an enhancement of nearly two orders of magnitude compared with traditional SIMS methods for the detection of polystyrene, a common organic polymer [29]. Metallization is especially useful for increasing the sensitivity for SIMS imaging of thick organic samples. Nevertheless,

ME-SIMS is still superior for the analysis of lipids and peptides. Several explanations for the sputtering mechanism of MetA-SIMS have been proposed. Metal cluster and nanoparticle formation may enhance the molecular ion yield and signal detection, by a number of proposed processes. First, the metallization of sample may eliminate sample charging due to the conducting paths created at the surface by the gold pattern. The elimination of charging effects induces a better-quality image [41]. Second, the metal clusters sitting on the surface of the sample can constitute a matrix that enhances desorption/ionization yield. Gold embedded in the sample acts as a cationing agent and may improve ion formation. Third, the metal evaporation by the primary ion beam may induce migration of mobile analytes onto metal nano-islands [29].

5.4   Analyzers to Improve IMS Capabilities

The mass spectrometry analytical technique combines sources and analyzers, which are interlocked and developed to increase the sensitivity and the number of parallel ion-detection events. Table 5.1 describes the different mass analyzer characteristics used for SIMS and MALDI imaging mass spectrometry. Different geometries of time-of-flight analyzers (linear, orthogonal, delayed extraction) and innovative mass analyzer instruments, such as quadrupole-TOF, ion mobility-quadrupole-TOF, and Fourier transform ion cyclotron resonance (FT-ICR), supply new perspectives and applications in imaging mass spectrometry [42–45].

In the early development of SIMS, the dynamic mode, which utilizes high-primary-ion current densities on the sample, was used due to limited sensitivity. The characteristic effect of the dynamic SIMS mode is typically increased erosion rates equivalent to the removal of up to several hundred monolayers of sample per second. Therefore, the instruments offered high detection efficiencies. Nevertheless, the dynamic mode is not suitable for the surface analysis of small areas and for long experiments. Thus, the static mode was developed by reducing the primary ion current density. At the first stage of static SIMS development, quadrupole and sector analyzers were combined to the SIMS source [46, 47]. These analyzers have a low transmission ratio (ratio of ions leaving a region of a mass spectrometer to the number of ions entering that region) and operate in a scanning mode. These properties resulted in limited sensitivity and unique m/z ion detection (low mass-resolving

Table 5.1 Characteristic performances of different mass analyzers

Analyzer	Mass-resolving power	m/z Range	Transmission	Detection	Sensitivity	Rep. rate
Quadrupole	10^2–10^3	10^3	0.01–0.1	Sequential	1	<1 Hz
Sector	10^4	>10^4	0.1–0.5	Sequential	10	<1 Hz
Time-of-flight	10^3–10^4	10^5	0.5–1.0	Parallel	10^4	>10 kHz
FT-ICR	10^4–10^6	10^6	0.2–0.9	Sequential	Zmol	<1 Hz

power), which results in the loss of important information for imaging MS experiments. The increased use of static SIMS in the 1980s [48] resulted in the replacement of quadrupole and sector mass analyzers with time-of-flight analyzers (ToF). TOF analyzers offer two main advantages: a theoretically unlimited mass range and a parallel mass registration, which allows for the collection of a mass spectrum at every image pixel (rapid data collection) [49–51].
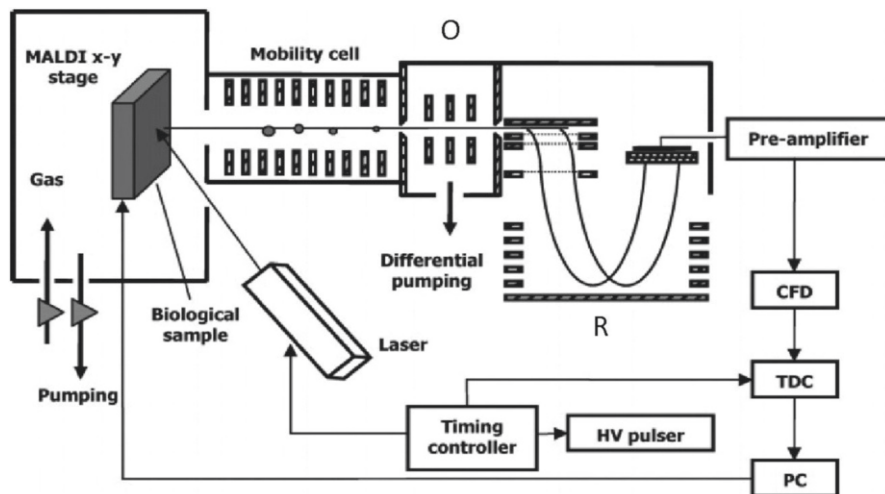
5.4.1   Time-of-Flight

Introduced by Stephens in 1946 [52], the time-of-flight analyzer has been combined with a SIMS ion source since the 1980s and with MALDI sources since its development in the early 1990s. ToF offers a good transmission ratio (50–100%), sensitivity, dynamic mass range, and repetition rate. The first high-mass-resolving power imaging with a ToF-SIMS instrument in a scanning microprobe mode was published by Schwieters' group in 1991 [53]. They reported secondary-ion images of a polymer with an average molecular weight of 1,400 m/z.

Rapidly, the efficiency and the utility of ToF-SIMS imaging were demonstrated by many experts who consider mass spectrometry the most powerful technique for chemical analysis. Since the 1990s, the SIMS and MALDI sources have been combined with different configurations of time-of-flight detectors.

Time-of-flight analyzers allow the separation of ionized accelerated molecules according to their molecular masses. Generated by the ionization beam in the source, ions characteristic of the surface species are accelerated by an electric field between the conductive support (and sample) and the extraction grid (10–25 kV) to the same kinetic energy. Therefore, the ions arrive at the detector with different speeds, which are inversely proportional to their mass over charge values. Three main ToF analyzer geometries are defined in order to increase the sensitivity, mass accuracy, and mass-resolving power. These entry geometries are linear, reflectron, and orthogonal.

The linear geometry is commonly used in ToF imaging mass spectrometry and provides the highest sensitivity. As shown in Fig. 5.5, reflector mode and a delayed extraction time can be performed to provide an increase in sensitivity, mass-resolving power, and mass accuracy. The reflectron is an electrostatic ion mirror placed at the end of the drift tube. The ion mirror reflects the ions and corrects the different velocities by focusing the ions with the same m/z value and improves the mass-resolving power. The delayed extraction time or pulsed ion extraction corresponds to a short period of time delay between firing the laser and extracting the ions, which improves the sensitivity and mass-resolving power of a MALDI experiment [54, 55]. The linear geometry with reflector mode and delayed extraction is widely used in imaging mass spectrometry [55]. Nevertheless, delayed extraction must be tuned for each mass and is less effective at high mass. Therefore, a second time-of-flight geometry, orthogonal acceleration, was presented by Guilhaus and coworkers [56]. This geometry, shown in Fig. 5.5, places the ion source orthogonal

Fig. 5.5 Mass spectrometer combined with an ion-mobility cell allows the separation of compounds according to their structure and conformation. In this example, an orthogonal time-of-flight (O) and electrostatic mirrors (R) as a reflector are used [43]

to the time-of-flight analyzer. This decoupling of the source from the mass analyzer results in an independent mass determination. The orthogonal mass analyzer allows a better mass accuracy in MALDI imaging as subtle height differences on the sample no longer influence the time-of-flight measured.

Previously used alone with a linear or orthogonal geometry, TOF mass analyzers are now combined with other mass analyzers in order to improve functionalities and capabilities. The quadrupole mass filter, developed in the mid-1950s by Wolfgang Paul, corresponds to four parallel hyperbolic rods that apply static or oscillating electrical fields to select ions. The quadrupole is well suited as an ion guide and collision cell to fragment parent ions and therefore allow molecule identification. The MALDI-Q-ToF mass spectrometer improves the capabilities of the MALDI imaging experiment by the localization, identification, and validation of molecules in tissue [44, 57].

5.4.2 New Instruments for Imaging Mass Spectrometry

The goal of developing imaging mass spectrometry is not to replace existing molecular imaging technologies but to offer an alternative detection method and the possibility of molecule identification directly on the tissue. Mass spectrometry is the instrument of choice for simultaneous localization and identification. To this end, new instruments with different mass analyzers have been developed to improve the selectivity, sensitivity, and identification of detected molecules. Fourier transform

ion cyclotron resonance (FT-ICR), microscope MALDI, and ion-mobility mass spectrometers are presented and discussed as new instruments for MALDI imaging mass spectrometry. FT-ICR and ion-mobility IMS increase the number of identified molecules in tissue samples [43, 58], whereas the microscope MALDI increases MALDI image resolution, down to 4 μm [7].

The MALDI–ion-mobility (IM)–orthogonal-time-of-flight mass spectrometer (oTOFMS) provides a gas-phase separation before the MS experiment. IM, also called plasma chromatography, was developed in the 1970s as a technique for ion separation [59]. IM applications range from protein interaction studies to conformer differentiation. Ion-mobility mass spectrometry (IMMS) consists of an applied electric field in a buffer gas to separate individual components according to their mobility differences (collisional cross section) followed by mass-to-charge ratio discrimination in a time-of-flight instrument. Flight times in the mass spectrometer are much shorter than residence times in the drift tube; thus, it is possible to record mass-resolved ion mobilities for all ions simultaneously [60]. The combination of IM and imaging mass spectrometry is especially well suited to discriminate lipids and peptides with the same mass-to-charge ratio [45]. Therefore, this separation allows simultaneous localization and identification [61].

The ultrahigh-mass-resolving power of MALDI FT-ICR reveals novel molecular distributions that remain hidden with low-resolution mass-spectrometric techniques [58].

The FT-ICR geometry was used in the early 1930s [62] for nuclear physics experiments and 40 years later for applications [63, 64]. The FT-ICR mass spectrometer is composed of an ion cyclotron resonance cell placed in a homogeneous high magnetic field. A Lorenz force perpendicular to the magnetic field causes the ions to rotate with a frequency that is inversely proportional to their m/z ratio. This frequency of rotation is measured as the induced charge on detection electrodes located on the ICR cell. The time-domain signal is measured, amplified, and Fourier-transformed to yield frequency-domain data and then converted to m/z [65, 66]. A longer time-domain signal yields a higher mass-resolving power and a more precise frequency determination, and thus a higher mass accuracy (Table 5.1). This increased mass-resolving power for MALDI imaging allows the identification and localization of more peptides and lipids in tissue. The main difference between FT-ICR and ToF is the delay time of mass analysis. In FT-MS, this period is much longer (ms to seconds) than in the ToF-MS (μs). Tissue digestion combined with ion mobility or FT-ICR mass spectrometry identifies a large number of peptides from different tissue types (formalin-fixed paraffin-embedded).

The microscope mode uses ion-optical microscope elements to project the spatial origin of the ions generated at the sample surface onto a two-dimensional position-sensitive detector [7, 67]. This approach of MALDI microscope mode imaging allows a 200-μm-diameter area analysis with a high spatial resolution (4 μm). In this case, the spatial resolution is independent of the spot diameter of the ionizing beam but depends on the quality of the ion optics and the detector. A single analysis over a large area now results in a higher efficiency of ion production as well as an increase in the temporal resolution. This mass spectrometer design allows for

the detection of compounds up to 4 kDa, such as lipids, peptides, and small proteins, which are of interest in lipidomics and proteomics. These applications are detailed later in Sect. 5.6 on the applications of surface-enhanced IMS.

Another technique describes a way to decrease the spatial resolution without modifying the ion optics. Microstructures of silicon wafer masks with small apertures were designed to decrease the laser diameter and the irradiated area. By application of these design masks close to the sample, 30-μm irradiated surfaces are easily obtained and can reach 10 μm without the loss of signal intensities [67, 68].

5.5   Sample Preparation and Protocols

The new fields of lipidomics and proteomics were born in the early 1980s when mass spectrometry (analytical chemistry) was applied to biological samples. The MS approach revolutionized molecular biology and biochemistry with its high sensitivity and high-throughput analysis. However, MS approaches involve stringent and precise sample preparation to avoid contaminants and false-positive detection of biomarkers. Due to the high sensitivity and the need for reproducibility, many congresses and initiatives are focused on standardizing the techniques [69, 70].

Sample preparation is one of the most important steps for sensitive, rational, and coherent analysis. The conditioning of the tissue and the timescale of the analysis are critical and were neglected in the past. Tissue samples are very sensitive to enzyme activity and surface contamination. After dissection, enzymes are still active and play a role in the degradation of the proteome and the transcriptome. New methods such as fast microwave irradiation and homogeneous heating have been used to prevent the degradation of proteins and peptides [71, 72].

Therefore, high reproducibility and standardization are essential prerequisites for any analytical approach. Moreover, maintaining the biochemical, molecular, and structural sample integrity is a crucial supplementary aspect for the field of IMS. These points are discussed here, from the tissue collection to the final analysis.

5.5.1   Tissue Collection

The first step of the IMS experiment is tissue collection, which is basically the application of the knowledge of anatomopathologists. The analysis of fresh tissue sections is not as difficult as that of preserved tissues. Frozen tissue and formalin-fixed and paraffin-embedded (FFPE) tissue are the two most common preparations used for the preservation of tissue integrity while avoiding molecular degradation. The analysis of archived specimens is widely restricted due to methylene cross-linkage between peptides and proteins [73]. However, recent FFPE tissue preparations have been presented and applied to proteomics studies [74, 75]. These new possibilities open the proteomics and imaging experiments to a large number of sample bibliotheca.

5.5.1.1 Fast Frozen Tissues

Generally, after an organ has been removed from a sacrificed animal or a biopsy has been taken, the sample is snap-frozen in isopentane (at −50 °C), depending on the volume of the tissue. Isopentane is preferred over liquid nitrogen (LN_2) due to its larger heat capacity, which prevents the formation of ice crystals in the tissue. Cooling down larger tissue volumes (such as entire organs) is more cumbersome due to the introduction of large temperature gradients. In those cases, LN_2 is often used. The formation of ice crystals can destroy the cellular morphology by disrupting the cell membranes. Different reports show the necessity to heat or to use microwave to inhibit the enzymatic activities and avoid protein degradation just after the animal sacrifice. In the past 10 years, an additional step of heating or microwave irradiation has been used to inactivate peptide and protein degradation [71, 72].

5.5.1.2 FFPE Tissue

Formalin-fixed and paraffin-embedded tissues are difficult to analyze by classical proteomics studies due to the cross-linkage between the amino and thiol groups of amino acids. A protocol with enzyme cleavage has been used to extract, detect, and localize protein fragments [76]. A dewaxing step with xylene and rehydration with graded water/ethanol baths are followed by applying enzyme on the sample surface using a microspotting technique. Enzyme spots with a 50–80-μm diameter allow a reproducible and controlled amount of deposited enzyme [74, 75].

5.5.1.3 Tissue Section

The biological tissue sample is cut at a temperature of −18/20 °C in a cryo-microtome following one of the previous sample-preparation steps. Samples embedding in embedding materials containing synthetic polymers such as polyethylene glycol (PEG) and polydimethylsiloxanes (PDMS) should preferably be avoided. These materials have a tendency to smear a thin layer of polymer over the sample surface during the sectioning procedure. This surface pollution often leads to preferential ionization and ion-suppression effects, which will reduce the resulting image quality. Clean tissue sections with a thickness of 10–15 μm are immediately deposited onto a stainless steel plate and directly analyzed or kept at −80 °C. The best extraction conditions and consequently the highest sensitivity and mass-resolving power are obtained when using stainless steel plates. However, other sample holders, such as a glass plate coated by a thin conductive layer, which allows staining optical image records, can be used. Just before analysis, the plates are warmed to room temperature and dried under vacuum. There is no delocalization of observed compounds (on the scale of a few hundred nanometers), regardless of their mass. Compounds such as phospholipids are unlikely to delocalize, but it is generally feared that light elements, such as Na^+ or K^+, can be rapidly delocalized on a

nanometer scale [1]. Nevertheless, no such movement of alkaline or organic ions has been observed at the micrometer scale under the conditions described above. In addition, this sample-preparation method is robust, reproducible, and easy and does not limit the lateral resolution.

5.5.2   Surface Modifications

5.5.2.1   Organic Solvent Treatment

Organic treatment consists of a step of fast solution application (chloroform, cold ethanol, water) on the tissue surface to remove a particular class of compounds (lipids or peptides) according to their solubilities in the solution used. The aim of this approach is to decrease the complexity of the sample and to avoid ion-suppression effects during the MS analysis. Many different sample preparations have been developed to increase sensitivity, such as washes with chloroform, methanol, water, or ethanol [77, 78]. These washes must be performed with caution to avoid any delocalization of hydrophilic peptides. Apolar solvents, such as chloroform or xylene, are used particularly to remove lipids and deconstruct the lipids layers of the cell membrane to increase the detection of high-mass proteins [74, 79]. Each sample is a unique model, and parameters must be optimized sample to sample. As shown in Fig. 5.6, analyses must be validated with immunochemistry to demonstrate that there is no delocalization of compounds after tissue preparation and treatment [79].

5.5.2.2   Matrix Deposition

Matrix-enhanced SIMS and MALDI techniques need a matrix deposited on the surface after sample sectioning and surface treatment. A large number of matrices and deposition techniques have been tested [28]. One of the key issues associated with ME-SIMS and MALDI is the selection of appropriate matrix material for different analytes according to the type of biological sample. Table 5.2 shows different matrices and their associated applications.

Generally, matrices are freshly prepared by dissolution in 50 % H_2O and 50 % acetonitrile to a concentration of 0.5 M. The goal of matrix application is to produce a very thin coating (several monolayers thick) on the tissue surface. Many techniques have been developed for matrix deposition without molecular delocalization, including spin coating, spraying, acoustic deposition, microspotting, and pipette depositing [74, 75, 85]. Pipette deposition and manual spraying were used for rapid analysis but are not suited for reproducible and accurate imaging experiments. However, the other techniques cited above (which have now been commercialized; the ImagePrep vibrational sprayer by Bruker Daltonics, the Portrait 630 acoustic spotter by Labcyte and the ChIP piezo spotting system by Shimadzu are a few
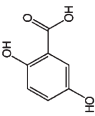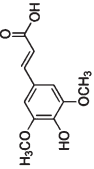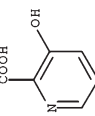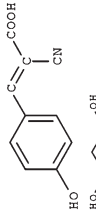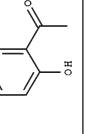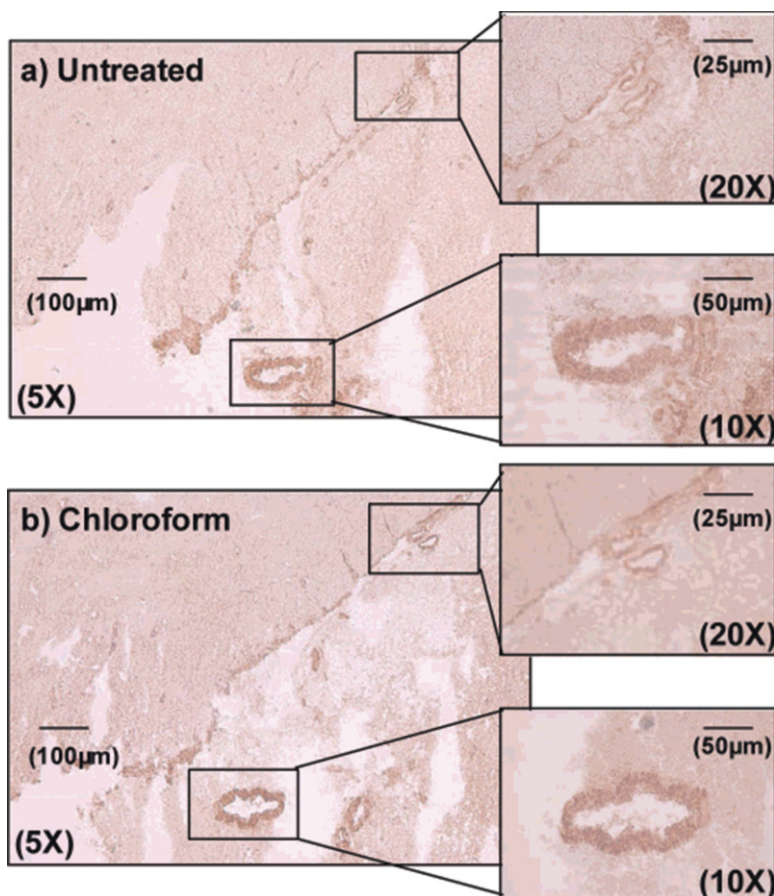
Fig. 5.6 Images obtained after immunochemistry of oxytocin peptides before (**a**) and after chloroform treatment (**b**) showing no delocalization of the peptide [79]

examples of available matrix-deposition systems) deposit matrix reproducibly with a well-known quantity and spot size (between 30–80-μm spot diameter). Ultimately, when a matrix deposition system is being used to enhance the molecular signal quality, the size of the matrix crystals will determine the obtainable spatial resolution and the sensitivity. Figure 5.7 provides an example where electrospray deposition was utilized to produce extremely small matrix crystals that are compatible with the spatial resolution of SIMS. Crystal sizes were smaller than 1 μm, as shown in Fig. 5.7c, allowing for the visualization of subcellular detail in these neuronal cells.

In this case of ME-SIMS, the dried droplet deposition should not be used, in order to avoid any peptide and/or biomolecule delocalization. Matrix droplets deposited on cryo-microtome cut tissue sections spread over the surface and crystallize. This leads to very large matrix crystal sizes (10 μm) and lateral analyte diffusion after wetting the tissue. Matrix solutions can be sprayed or deposited with a very small droplet diameter (90 μm) to avoid diffusion of molecules over the sample.

Table 5.2 Common matrices used for matrix-enhanced mass spectrometry techniques and their associated applications

Compound	Name	Structure	Solvents	Applications
DHB	2,5- Hydroxybenzoic acid		Acetonitrile, water, methanol, acetone, chloroform	Peptides, proteins, lipids, glycoproteinsglycanes [30, 80]
SA	3,5-Dimethoxy-4-hydroxycinnamic acid		Acetonitrile, water, methanol, acetone, chloroform	Proteins [78, 81], glycoproteins
3-HPA	3-Hydroxypicolinic acid		Ethanol	Alcalins, oligonucleotides, proteins [82, 83]
HCCA	a-Cyano-4-hydroxycinmamic acid		Acetonitrile, water, ethanol, acetone	Lipids, peptides [39], proteins [84]
THAP	2,4,6-Trihydroxy acetophenone		Ethanol	Oligonucleotides, peptides

Fig. 5.7 Scanning electron
microscopy images of
Lymnaea stagnalis nervous
tissue (**a**) prior to matrix
application (scale bar 10 μm)
and (**b**) after electrospray
deposition of 2,5-DHB
(scale bar 10 μm);
(**c**) higher-magnification
image showing submicron
crystal dimensions
(scale bar 1 μm) [86]
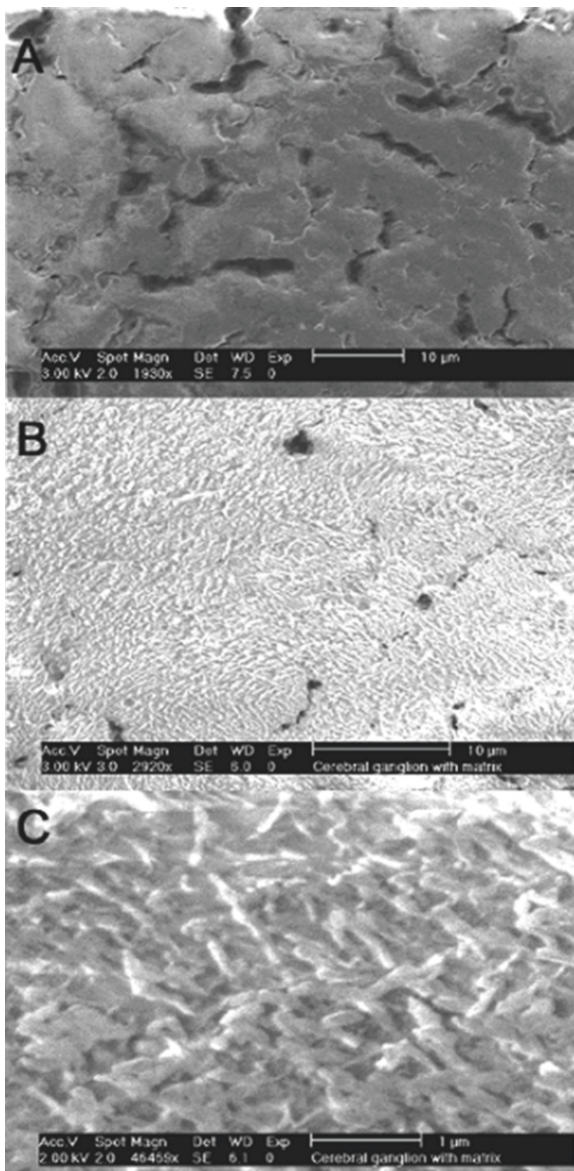
5.5.2.3 Metal Deposition

Metal deposition consists of a unique surface modification (MetA-SIMS) or
sometimes an additional step for MALDI ionization or ME-SIMS ionization
enhancement and will be discussed in detail in the next section.

Metal deposition is realized using metal-coating techniques similar to those used in electron microscopy. This provides a reproducible and accurate deposition of metal to the sample surface. Usually, a thickness of 2–5 nm is deposited and increases the ionization efficiency up to 3 kDa [40, 41]. The metal thickness is determined during the deposition process using a quartz crystal microbalance integrated in the metal-deposition system. Studies using atomic force microscopy indicated that during 1–2-nm gold deposition small islands are formed on the tissue surface. The surface becomes conductive although it is difficult to exactly assess the conductivity of the ITO–tissue–Au sandwich structure. If the thickness exceeds 5 nm, many gold clusters are formed and the molecular signal is suppressed completely. This is believed to indicate the formation of a solid, closed film that minimizes energy deposition directly in the tissue.

5.5.3   Comparison of Metallization and Matrix-Deposition Procedures

Metallization and matrix deposition enhance ionization and desorption, but these processes do possess drawbacks. Here, we will recapitulate a series of criteria, which are initiated from the personal interpretation of Delcorte [87] and applied to MALDI and SIMS imaging experiments. The interpretation and coherence of the imaging results are correlated to different criteria of efficiency, reproducibility, versatility, and ease of interpretation, as summarized in Table 5.3.

Efficiency is characterized by an enhanced ionization yield, which is comparatively the same in MetA-SIMS and ME-SIMS. However, the dynamic mass range of the MetA-SIMS procedure is more limited (up to ~ 3 kDa) than that of ME-SIMS [40].

Reproducibility is the major factor for imaging techniques to obtain coherent observations. The reproducibility of imaging MS experiments is characterized by two main aspects: the detection and localization of identical intensity signals. The reproducibility of matrix deposition is less effective than metal deposition due to the difficulty to reproduce the same deposition conditions and matrix crystal size/structure [86, 88, 89]. Nevertheless, many different matrix-deposition methods have been developed to reproduce the same quality of coverage and allow more

Table 5.3 A comparison between surface metallization and matrix deposition for SIMS-based tissue imaging mass spectrometry

Criterion	Matrix deposition	Metal deposition
Efficiency	++	++
Reproducibility	−	+
Versatility	+/−	++
Ease of interpretation	−	+
Equipment/cost	+	−

++ very good, + good, +/− satisfactory, − limiting

reproducible images. Moreover, the crystal size (around 1–5 μm) does not have the same effect in SIMS and MALDI imaging, with regard to the beam diameter. In the case of MALDI, the laser beam could reach 20 μm, and the image does not have enough spatial resolution to be affected by the crystal size. However, in SIMS a smaller beam (500 nm) is used and quality of the images is restrained to the crystal size. In addition, matrix deposition induces an increase in low-mass-range matrix signals, which interfere with sample signals, unlike metal deposition.

Versatility defines the number of possible applications of SIMS and MALDI imaging with metal or matrix deposition. Metal deposition allows a large number of applications because of its accurate deposition for any type of sample surface without any delocalization [30]. Moreover, the interpretation of their spectra is easier because only peaks from the metal are detected [90]. In the case of a matrix-enhanced SIMS experiment, the matrix produces interference in the spectra [91].

5.6   Applications of MALDI and Enhanced SIMS Imaging

Chemical imaging mass spectrometry provides both chemical information and the spatial organization of each component on a surface. The development of imaging mass spectrometry is revolutionizing the field of biological analysis [92]. SIMS and MALDI are the two most common techniques for the characterization and localization of compounds and provide a broad spectrum of applications.

The first analyses of biological tissue used a SIMS mass spectrometer for metal, lipids, and peptides localizations [93] with a high spatial resolution of 0.5 μm. A high spatial resolution combined with a high sensitivity for high-mass molecules remains the goal of chemical imaging mass spectrometry. Both MALDI- and SIMS-based approaches have been developed to achieve these goals, as discussed above.

Three large families of molecules are implicated in the organization (structure and activity) of cells: proteins, lipids, and carbohydrates. These biomolecules are observed at different concentrations (10^6 of magnitude) in the tissue, have different biochemical properties (molecular weight, pH iso-electric, proton affinity), and result in a different degree of desorption and ionization efficiency. The key to success is to apply appropriate imaging techniques (IMS and traditional imaging techniques) to answer a precise question.

In this section, we present different applications of molecular imaging mass spectrometry in the detection of molecules [such as pharmaceuticals, metabolites, atoms (metals), lipids, peptides, and proteins], that play a role in disease or specific conditions from plants to animal tissue. The choice of the complementary IMS technique depends on two parameters: the nature of the detected compounds (and the correlated mass) and the spatial resolution. The surface enhanced IMS helps to understand the role of each molecule in many different fields of research (lipidomics, proteomics, clinical proteomics, and pharmacology), showing a large spectra of applications.

5.6.1 Single-Cell Imaging of Peptides and Lipids for Fundamental Biological Studies

Surface-enhanced SIMS is the suitable instrument for the detection of low-mass molecules such as lipids and small peptides. Moreover, the detection of molecules in ganglia samples of small animals requires a high spatial resolution; thus, SIMS could play an important role for high spatial localization of biomolecules without chemical labeling (as is required in immunochemistry or targeted approaches).

Recent studies have combined surface-enhanced SIMS and MALDI to detect and localize compounds in biological samples. Heeren's group developed and applied surface analysis using ME-SIMS and MetA-SIMS for the detection of neuropeptides and lipids in *Lymnaea stagnalis* [86] and neuroblastoma [3].

Matrix (2,5-dihydrobenzoic acid in these examples) was deposited by an electrospray-deposition (ESD) system in order to ensure small matrix crystals compatible with the high spatial resolution of SIMS (Fig. 5.7). After tissue sectioning and pickup, the *Lymnaea stagnalis* tissue was sectioned with a cryo-microtome, placed on an indium-tin-oxide (ITO) coated glass slide, and coated with DHB matrix by ESD. The tissues were analyzed on a TRIFT-II time-of-flight SIMS (ToF-SIMS) equipped with an ^{115}In$^+$ liquid metal ion gun (LMIG), and on a MALDI equipped with 337 nm nitrogen laser VSL-337i in reflectron mode.

Different peptide and lipid profile images produced from SIMS and MALDI mass spectrometry were compared to scanning electron microscopy (SEM) images [86]. SEM was used to determine the size of the matrix crystals, thus validating ESD for ME-SIMS matrix deposition. The crystal size was ~1 µm, which allows imaging at subcellular resolution. ME-SIMS and MALDI spectra show peaks under 3,000 m/z (Fig. 5.8), which reveal the presence of the neuropeptide APGWamide in the anterior lobe of the right cerebral ganglia (Fig. 5.8) in the associated images (Fig. 5.9). This peptide regulates the male copulation behavior of *Lymnaea stagnalis* [94]. This study corroborates previous studies of matrix-enhanced SIMS and shows the power of ME-SIMS to detect and image both lipids and localized neuropeptides with a high spatial resolution (1.5 µm).

Surface metallization was used as an alternative to matrix deposition with SIMS and added (in addition to the matrix) for MALDI analysis. High-resolution images of lipids and peptides were obtained for neuroblastoma cells and rat brain tissues with MetA-SIMS, ME-SIMS, and a homemade MALDI-BioTRIFT instrument with a higher spatial resolution than commercially available MALDI instruments [7, 30].

ME-SIMS increases the signal intensities for phospholipids, phosphatidyl choline (PC), sphingomyelin (SM), cholesterol, ceramide, and di-acyl glycerol (DAG) (Fig. 5.8) compared to regular SIMS analysis. MetA-SIMS further increases the same signals (~50×) and also increases the yield of other molecular signals, as shown in Fig. 5.10.

Lateral resolution analyte diffusion is minimized in MetA-SIMS, where only migration on gold islands at the nanometer scale may occur, which produces
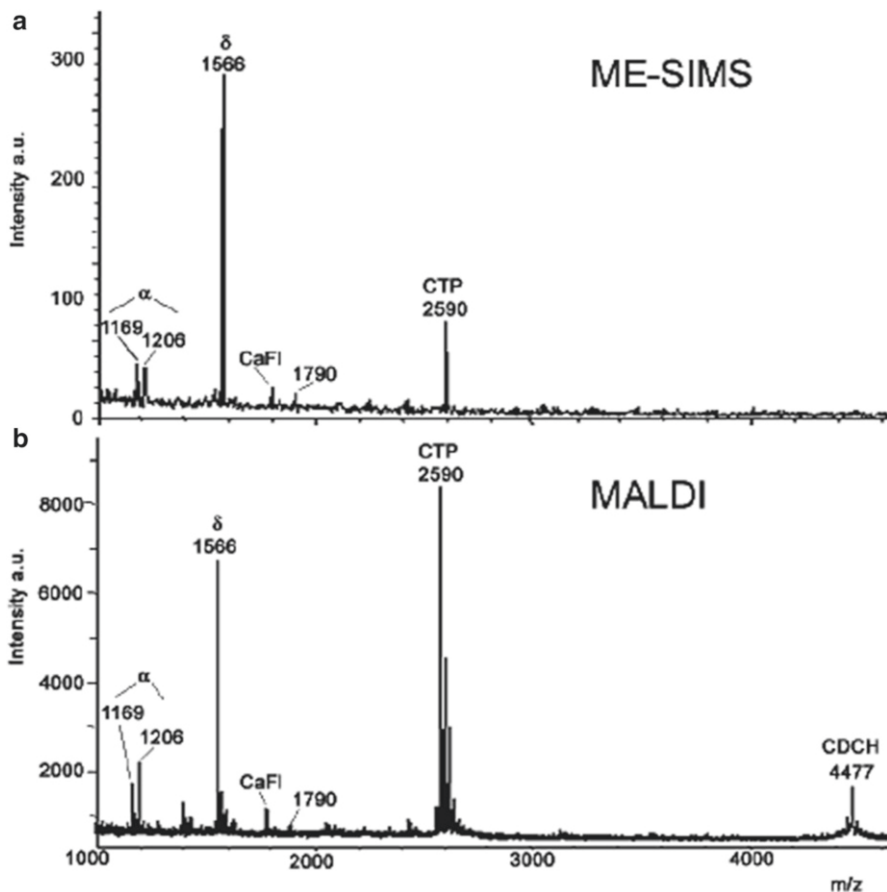
Fig. 5.8 ME-SIMS vs. MALDI: (**a**) ME-SIMS and (**b**) MALDI spectra of a commissure extract of the pond snail *Lymnaea stagnalis*. Both spectra were obtained using standard dried droplet sample preparation with 2,5-DHB as matrix. The peptides identified are R-caudorsal cell peptide (R, protonated and cationized), ä peptide (ä), HFFYGPYDVFQRDVamide (*m/z* 1,790), Calfluxin (CaFl), carboxyl terminal peptide (CTP), and caudodorsal cell hormone (CDCH). The ME-SIMS measurements used indium primary ions (total ion dose 8.9×10^{11} ions/cm^2) and the MALDI experiments 250 shots of the 4-ns 337-nm nitrogen laser [80]

better-quality images than ME-SIMS. Moreover, higher mass signals are observed (peptides) up to 1,400 Da. The combination of the spatial resolution and the high sensitivity for cholesterol and other ions allows the description of subcellular organization and the differentiation of cell clusters of the neuroblastoma. The membrane, nucleus, and intracellular compounds are observed to delineate the neuroblastoma.

Moreover, except for the lipids' signals, the spectrum shows no other molecular signals in ME-SIMS, while signals up to 4,000 and 1,500 Da are observed from the
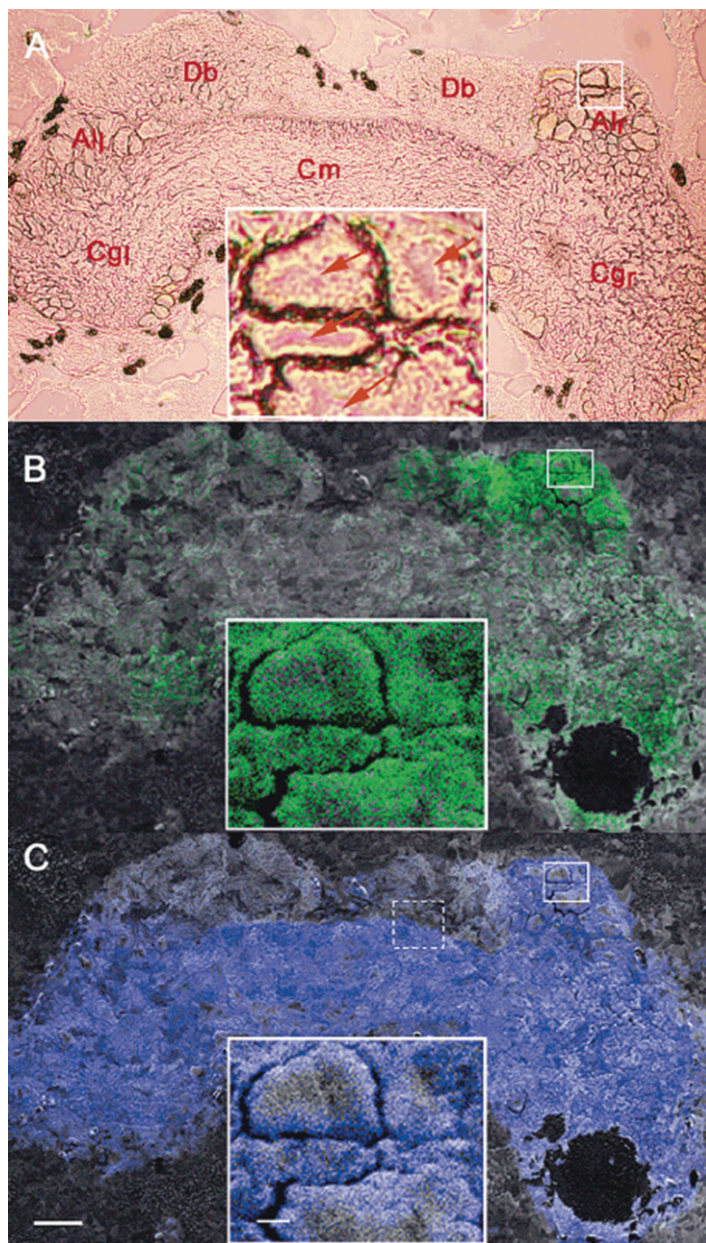
Fig. 5.9 Direct molecular imaging of *Lymnaea stagnalis* nervous tissue by ME-SIMS:: (**a**) optical image of the *Lymnaea* cerebral ganglia; inset shows high-magnification image of neurons in the anterior lobe (*solid box*); *arrows* indicate nuclei. Different regions in the section are right and left cerebral ganglia (Cgr and Cgl), anterior lobe (Al), commissure (Cm), and dorsal bodies (Db); (**b**) ME-SIMS image of APGWamide (429.0–433.2 *m/z*; *green*) distribution; (**c**) ME-SIMS image of cholesterol (368.2–371.3 *m/z*; *blue*) distribution. Scale bar: 200 μm; scale bar inset: 10 μm. Molecular images (**b** and **c**) are presented as colored overlays on top of the gray-scale TIC (total ion count) image (mass range: 1.0–5,000 *m/z*) [3]
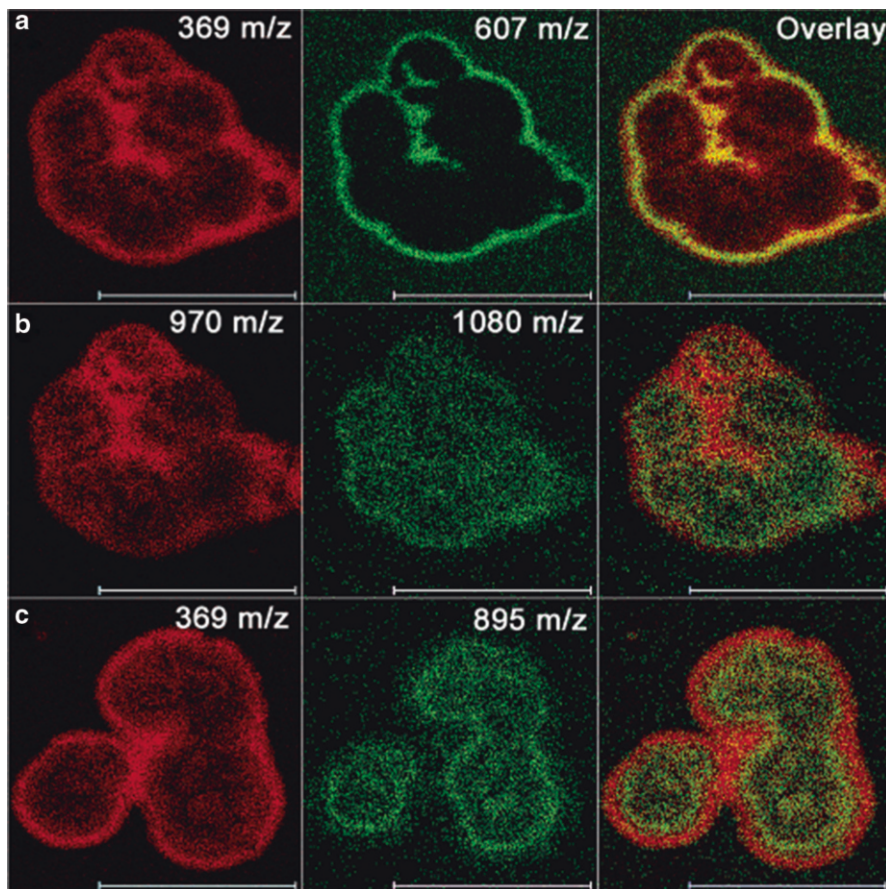
Fig. 5.10 Cellular localization of MetA-SIMS selected ion count signals from neuroblastoma cells. Cells were imaged after deposition of 1-nm gold: (**a**) *m/z* 369 (cholesterol [M–OH]+, 0–14 counts) and 607 (DAG, 0–6 counts); (**b**) *m/z* 970 (cholesterol [2 M + Au]+, 0–4 counts) and 1,080 (0–1 counts); (**c**) *m/z* 369 (cholesterol [M–OH]+, 0–12 counts) and 895 (0–2 counts) [3]

same section by stigmatic MALDI and MetA-SIMS. These results are explained by the major difference between the two approaches, which relates to the amount of sample consumed. In MALDI, each laser shot consumes approximately 100 nm–1 μm of sample, while the penetration depth of the SIMS is typically 10 nm. This is explained by the crystallization and segregation of lipids on the crystal surface of the matrix, while the peptides are mainly incorporated into the matrix [95].

Sample preparations of tissue with chemical modifications used with the MALDI-BioTRIFT technique show high-mass signals up to 4,000 Da, with a higher spatial resolution (approximately 2 μm). Gold deposition results in an enhanced image quality and signal intensity, not only for SIMS but also for MALDI.
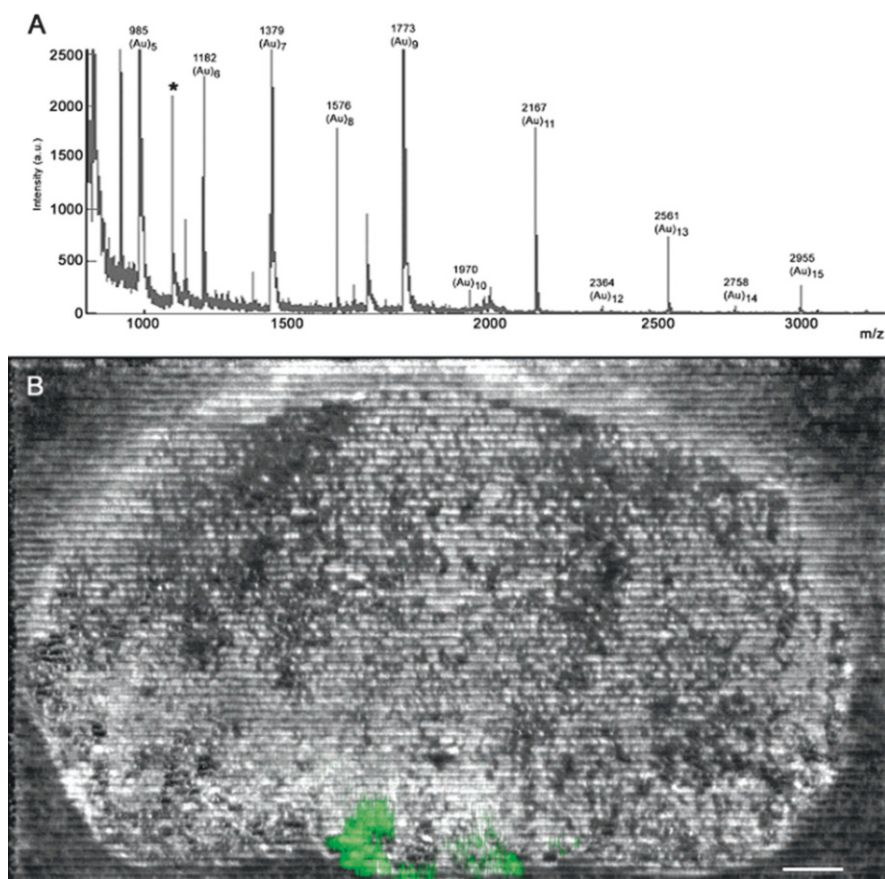
Fig. 5.11 MALDI stigmatic imaging of a rat brain tissue section: (**a**) a line scan summed mass spectrum showing gold cluster peaks and several peptide peaks, with the vasopressin mass at *m/z* 1,085 (*); (**b**) TIC image (gray scale) of an HCCA-coated rat brain tissue section overlaid with the selected ion image for vasopressin (*green*). Scale bar: 1 mm [3]

Figure 5.11 shows images of a localized vasopressin (1,085-Da) protein obtained from matrix-enhanced MALDI.

ME- and MetA-SIMS describe localized low-mass signals from lipids and peptides by the assistance of chemical modifications. The matrix deposition for ME-SIMS is the prerequisite for MALDI analysis as well. MALDI allows the multimolecular imaging of peptides and proteins up to 75 kDa. The large dynamic mass range allows for the analysis of complex mixtures of compounds in tissues and has many biological applications. Applications include imaging of organs or whole animal body slices as well as vegetable models [11, 96], with the detection and localization of drugs, metabolites, peptides, proteins, and carbohydrates.

### 5.6.2   Peptide and Protein Detection: MALDI Imaging Applications

The first direct image construction by MALDI was initiated by Caprioli's group [11]. At this juncture, in 1997, MALDI was described as a technique to analyze a biological solution with proteins and peptides. Different groups have applied this technique to a direct analysis of tissue by matrix droplet deposition followed by MALDI-ToF MS analysis [97–99]. Different average spectra for regions of interest (ROI) are compared and allow differentiation of the proteome and lipidome in certain regions.

In the past decade, many developments for sample preparation, instrumentation optimization, and software have enabled MALDI imaging at a subcellular resolution with good sensitivity [80].

5.6.3   Proteomics and Clinical Proteomics

No specific sample-preparation methods were used for the first MALDI imaging experiments. The matrix was applied directly with a pipette or spayed onto the tissue in order to make a reproducible procedure to detect some standard peptides and proteins [11, 100, 101]. The choice of a spraying system or microspot deposition of matrix is crucial for the spatial resolution and the reproducibility of experiments. The mass range detectable with MALDI imaging is approximately 0–80 kDa. The first application of MALDI on a biological surface was to detect large molecules for proteomics studies (Fig. 5.12) [102]. In this case, human glioblastoma cells were implanted into a hind limb of a nude mouse model and specific markers (Tβ.4 protein, $m/z = 43{,}965$) were observed in the tumor proliferation area (Fig. 5.12). These first publications illustrate the interest in MALDI imaging for proteomics and clinical proteomics research: detecting proteins implicated in disease pathologies, that discriminate different cell or organ states.

The work of the Sweedler group illustrates the usefulness of MALDI imaging in the neuroscience field [103–105]. The Sweedler group has developed methodologies and sample preparations for invertebrate ganglia cell imaging. The application of matrix onto the *Aplysia californica* exocrine gland and neuronal tissue shows the ability to spatially image neuropeptides and proteins. Two different approaches have been used. First, a microspotted matrix deposition on different ganglia slides (every 30 μm) demonstrated the ability to profile neurons without removing cells from the ganglion matrix from the ventral to the dorsal side. Another approach uses total laser ablation of the matrix and moves the plate a distance (25 μm) smaller than the laser spot size, a so-called oversampling approach. In this manner, even with a large laser spot, a small analytical area can be studied, improving the spatial resolution of the resulting image. The use of an adequate bioinformatics tool to reconstruct the image allows the imaging of molecules with a resolution of 50 μm.
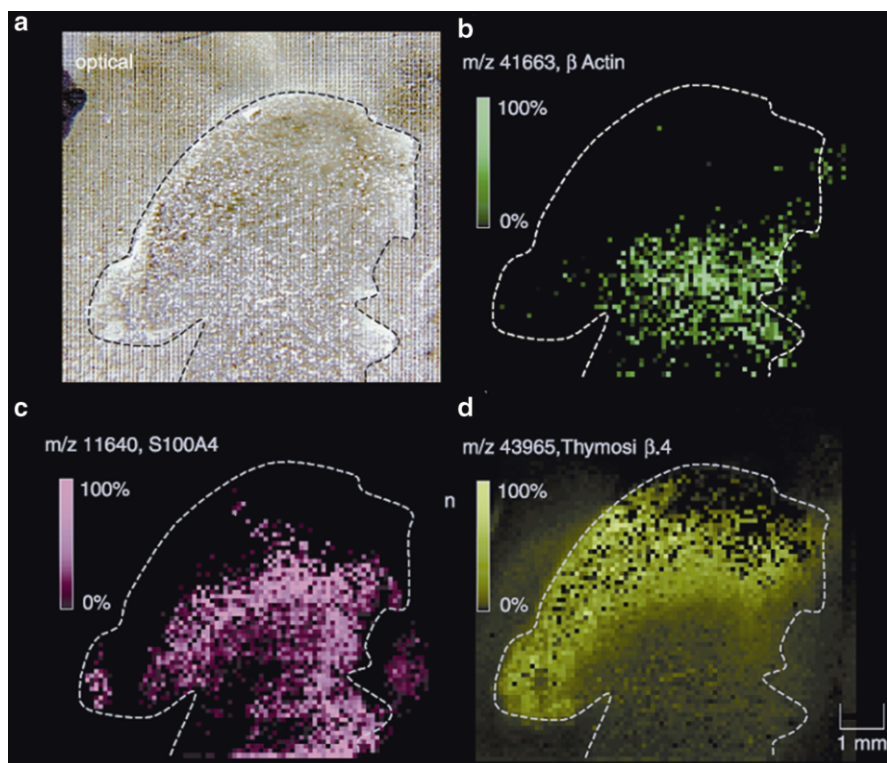
Fig. 5.12 Selected protein images from a glioblastoma section: (**a**) human glioblastoma slice mounted on a metal plate, coated with matrix (the lines are from ablation of matrix with the laser); (**b–d**) mass-spectrometric images of proteins showing a high concentration in the proliferating area of the tumor (**d**) and other proteins present specifically in the ischemic and necrotic areas (**b** and **c**) [102]

At the same time, other groups have applied MALDI imaging to different diseases by integrating sample comparisons [78, 81, 106, 107]. As illustrated in these papers, MALDI mass-spectrometric imaging on tissues is used in endogen biomarker discovery by determining under- and overexpressed peptides/proteins of a disease state versus a healthy control (AD). MALDI mass-spectrometric imaging has also been applied to the study of amyloid beta peptide distribution in brain sections from mice and shows features reminiscent of Alzheimer's disease.

5.6.4 Drug Distribution and Quantification

IMS has also been used to observe the elimination and repartition of drug distributions on tissue sections [44, 78, 96, 108–111]. The drug profile and ADME (adsorption, distribution metabolism, and excretion) studies appear to be particularly well
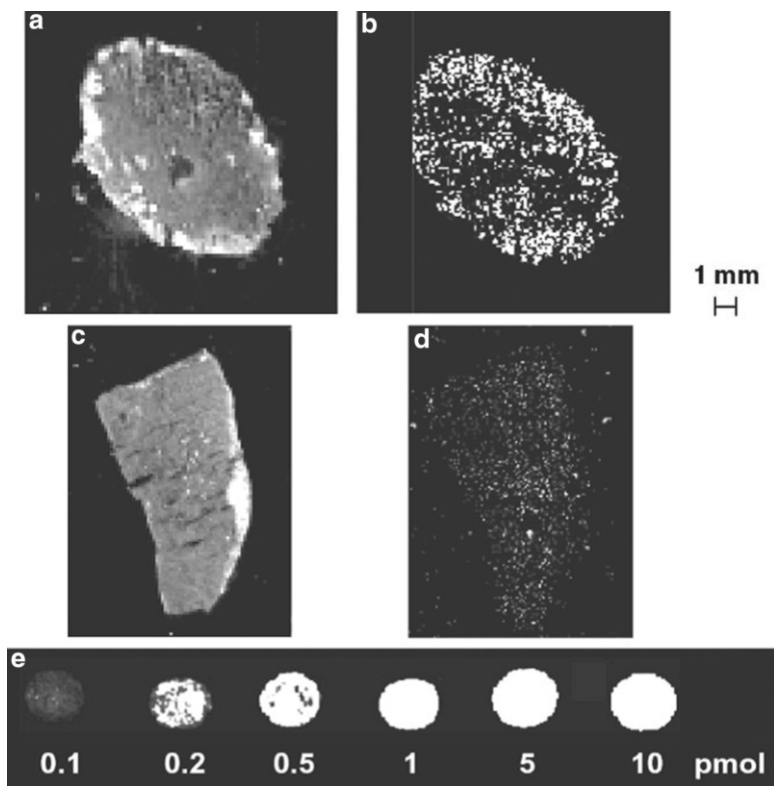
Fig. 5.13 Drug distribution of erlotinib in rat liver (**a**, **b**) and spleen (**c**, **d**) tissue section. (**a**) and (**c**) represent the optical image, while (**b**) and (**d**) represent the MALDI image of erlotinib at $m/z = 278.1$. (**e**) represents the dilution series of erlotinib on target plate as a calibration (the HCCA matrix was deposited by hand) [78]

suited with IMS [57, 109, 112]. In these articles, different drugs are injected into the animals, and monitored by single-MS or tandem-MS imaging to visualize the drug incorporation. Signor et al. compared the quantification of erlotinib by autoradiography, LC-MS, and MALDI imaging experiments. As shown in Fig. 5.13, at a concentration of 3.76 ng/mg, erlotinib and its metabolites are observed in the rat liver and spleen sections. The comparison of quantification techniques (autoradiography and LC-MS/MS) was also similar with MALDI analysis as a quantitative approach [78].

However, signal intensities may vary even in the same sample; thus, MALDI MS is not the method of choice for absolute quantification. In this study [112], the drug distributions and the intensity ratios could be reproduced within a range of 20 % (if the sample-preparation procedure as well as instrument settings and laser intensity are kept constant). An internal calibration and reproducible deposition of matrix enable relative quantification with the comparison of peak areas instead of height peaks.

Several groups have shown that this method allows a quantification error variation of about 2–3 % [96, 113, 114]. New methods such as multiple reaction monitoring (MRM)–based imaging on triple quad systems provide a rapid, more sensitive targeted analysis of drug distributions in whole body tissue sections [115]. Although these methods are relevant to quantify sample-to-sample variations, validation processes are still used with established methods such as Western blot and immunochemistry for determining accurate concentrations. It is necessary to combine IMS with HE staining and immunohistochemistry to validate IMS as an approach for the identification of molecules from tissue [116]. Thus, a validation method was developed with a tag-mass, called specific mass spectrometry imaging. This approach allows the simultaneous detection and validation of molecules of interest using IMS [81, 83, 107].
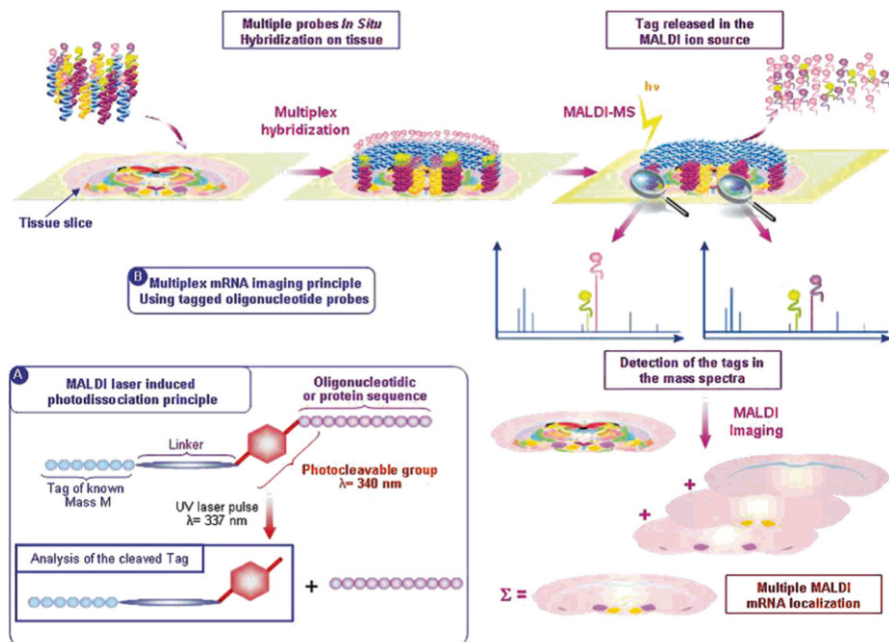
5.6.5 Specific Mass Spectrometry Imaging

Specific mass spectrometry imaging is used to image different types of molecules, such as proteins and nucleotides, with a combination of mass spectrometry imaging and immunohistochemistry. A tag-mass is used, which is a tagged antibody or aptamer that can be observed in the IMS experiment. This concept was developed to detect compounds such as nucleotides and large proteins, which are difficult to ionize by classical IMS experiments. A specific mass spectrometry imaging experiment is shown in Fig. 5.14 along with the different steps of tag-mass multiplexing.

5.6.6 Application with Carbohydrates and Metabolites in Plants

IMS applications in the vegetable kingdom, including MALDI imaging of oligosaccharides and primary metabolites in a plant system, have recently been presented [117]. MALDI imaging was used to identify metabolites, namely, glucose-6-phosphate, in potato tubers [118] and to determine agrochemical compounds in soybeans [119]. In these examples, the sensitivity of MALDI imaging and the semi-quantitative evaluation allow the detection of hundreds of metabolites with a concentration of around 1 μg/g. Other approaches, including electrospray mass spectrometry and enzyme-linked assay, could be combined with IMS, but the sensitivity of IMS offers the potential of simultaneous metabolite assays. Nevertheless, there are over 100,000 plant metabolites, and MS/MS is necessary for accurate identification. Combined IMS and MS/MS approaches have been developed for frozen, fixed, and embedded tissues [120]. These methods will be discussed in the section entitled "Perspectives" ahead.

Recently, Thomas-Oates published a study on the localization of carbohydrate metabolites as an indicator of grain yield. Cross and longitudinal sections from the

Fig. 5.14 Specific mass spectrometry imaging approach uses a tagged reporter, which allows the multiplex detection of a large number of molecules, including nucleotides and proteins. In this example, the tag-mass is a complementary oligonucleotidic sequence, which has a high affinity to the complementary sequence of interest in the tissue. This affinity and the IMS experiment allow the localization of the interest sequence of DNA, RNA, or proteins in a more general aspect [83]

wheat stems of *Triticum aestivum* were used to localize water-soluble carbohydrates [121]. They demonstrated the sensitivity of IMS and verified the results using complementary techniques, including LC-MS. An advantage of IMS over the other techniques included the ability to determine *in situ* localization.

5.6.7 MALDI Imaging of Lipids

Lipid distributions are usually detected and mapped by SIMS mass spectrometry, especially because of the sensitivity to SIMS in the low-mass range. Lipids can also be detected and localized by MALDI with special matrices to minimize interference from matrix peaks. In this context, the MALDI ion-mobility mass spectrometry imaging technique was developed. MALDI-Q-ToF, coupled with an ion-mobility cell, developed by the groups of Woods and Schultz, allows for the separation of lipids, matrix, and peptide species [43, 45, 122]. This separation allows a differentiation between species, with a higher signal-to-noise ratio, as shown in Fig. 5.15.
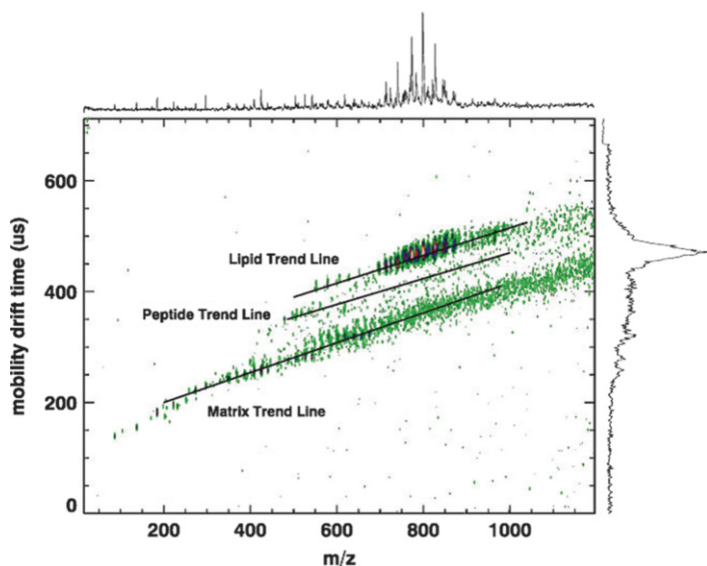
Fig. 5.15 Ion-mobility diagram obtained by MALDI-IM imaging of a rat brain section. The *y*-axis is the time separation in the drift cell, and the *x*-axis is mass-to-charge ratio. Different species (here, DHB matrix, peptides, and lipids) fall on unique trend lines [45]

5.6.8   Element/Metal Detection

One other dedicated application of IMS is the localization of contrast agents used for MRI imaging [123–125]. Contrast agents, used to increase the contrast of images during in vivo imaging by MRI or PET instruments, were studied by IMS to accurately localize their distributions in organs and cells with a better sensitivity and spatial resolution than classical MRI. In these examples, IMS allowed the detection of contrast agents in their native or degraded form [126].

5.7   Perspectives

As presented here, surfaced-enhanced SIMS and MALDI imaging are two recent approaches to detect and image macromolecular compounds directly in biological samples. Important recent developments include sample-preparation protocols and, in particular, instrument combinations of SIMS and/or MALDI ionization sources with different mass analyzers. These developments are correlated to the same developments observed in classical proteomics studies many years ago. In that sense, it is easy to foresee the inclusion of IMS into biological studies.

In a general view, IMS is able to visualize different compounds with a spatial resolution of 50 nm–100 μm with good sensitivity. Nevertheless, the accurate identification and validation of these compounds is still difficult. In this way, many different approaches, such as immunochemistry and autoradiography, validate the presence of biomolecules. In the past decade, different tandem mass spectrometry (MS/MS) approaches were developed with instruments with new geometries to directly identify molecules in tissue [127]. These new geometries allow a better separation and possible *in situ* identification of compounds such as lipids and digested proteins. Thus, two groups have developed *in situ* enzymatic digestion to map large proteins in frozen and formalin-fixed and paraffin-embedded (FFPE) tissues [74, 75, 128].

Trypsin digestion (from classical proteomics experiments) on FFPE tissues allows proteomics studies on archived tissues from hospital libraries [76]. This method of digestion requires a micro-deposition instrument to avoid any delocalization of digested peptides, where trypsin deposition comes before matrix deposition. Digestion on tissue allows the identification and localization of thousands of digested peptides. Nevertheless, it is difficult to identify all of the fragments because of the high concentration of peptides and lipids in the mass range of 350–950 m/z. In this perspective, digested FFPE and frozen tissues were analyzed with an ion-mobility mass spectrometer [128]. This approach separates molecules (e.g., peptides, drugs, and proteins) according to their conformation (cross section) and offers better identification. Moreover, MALDI ion-mobility imaging allows the separation of drugs from lipids, saccharides, nucleotides, and peptides. The use of standard protocols, coupled with sensitive instruments that can separate ions in the gas phase prior to mass analysis, could be the way to improve the field of imaging mass spectrometry.

5.8 Conclusion

As shown in this chapter, surface-enhanced imaging mass spectrometry and IMS are technologies based on fundamental innovations in physics and chemistry. Their applicability to biological and biomedical studies has been shown. SIMS and MALDI combined offer complementary surface-analysis approaches to study a range of species, from elements to proteins (Fig. 5.16). Applications include biomarker discovery or drug assessment (ADMET: absorption, distribution, metabolism, elimination, toxicology) on biopsy surfaces. As a result, this method can be involved in each step of drug discovery: for target identification, lead optimization, assessment of drug-delivery systems, and profiles of the biodistribution and metabolism.

These young techniques are under development to increase their sensitivity, speed of analysis, reproducibility, and spatial resolution. The numbers of papers published recently demonstrate the power and potential of these approaches to overcome "classical" imaging problems. Initially developed to localize lipids, peptides,
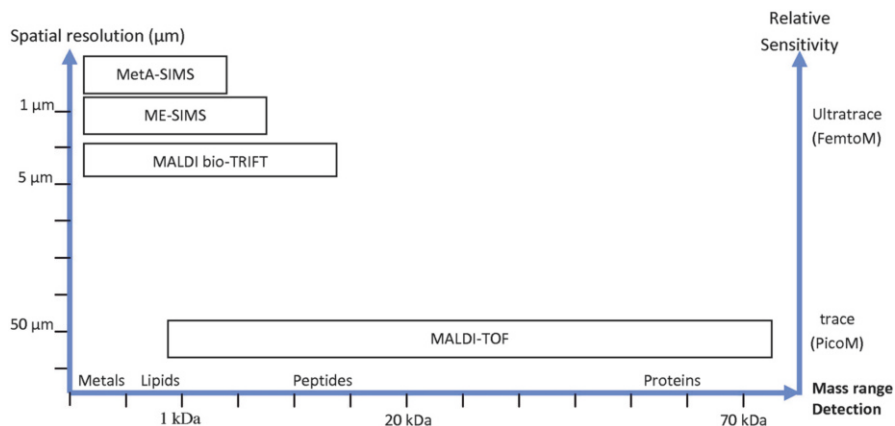
Fig. 5.16 Description of the different enhanced-surface IMS techniques according to their spatial resolution, mass-range detection, and sensitivity

and proteins, MALDI imaging and surface-enhanced SIMS allow the detection of biomarkers related to specific tissue conditions.

Imaging mass spectrometry is a label-free imaging technique for molecular pathology that complements existing, less specific imaging modalities in biomedical research. This innovative MS-based technique, together with such techniques as MRI, CT, PET, or ICC imaging, will visualize the fundamentals of diseases in future biomedical imaging research.

References

1. McDonnell LA, Heeren RMA. Imaging mass spectrometry. Mass Spectrom Rev. 2007;26: 606–43.
2. Castaing R, Slodzian G. Microanalyse par emission ionique secondaire. J Microsc. 1962;1: 395–410.
3. Altelaar AFM, Klinkert I, Jalink K, De Lange RPJ, Adan RAH, Heeren RMA, Piersma SR. Gold-enhanced biomolecular surface imaging of cells and tissue by SIMS and MALDI mass spectrometry. Anal Chem. 2006;78:734–42.
4. McDonnell LA, Heeren RMA, de Lange RPJ, Fletcher IW. Higher sensitivity secondary ion mass spectrometry of biological molecules for high resolution, chemically specific imaging. J Am Soc Mass Spectrom. 2006;17:1195–202.
5. Altelaar AFM, Luxembourg SL, McDonnell LA, Piersma SR, Heeren RMA. Imaging mass spectrometry at cellular length scales. Nat Protoc. 2007;2:1185–96.
6. Heeren RMA, McDonnell LA, Amstalden ER, Altelaar AFM, Piersma SR. Why don't biologists use SIMS; a critical evaluation of imaging MS. Appl Surf Sci. 2006;252:6827–35.
7. Luxembourg SL, Mize TH, McDonnell LA, Heeren RMA. High-spatial resolution mass spectrometric imaging of peptide and protein distributions on a surface. Anal Chem. 2004;76: 5339–44.

8. Klerk LA, Lockyer NP, Kharchenko A, MacAleese LP, Dankers PYW, Vickerman JC, Heeren RMA. C_{60}^+ secondary ion microscopy using a delay line detector. Anal Chem. 2010;82: 801–7.

9. Karas MI, Bachmann D, Bahr U, Hillenkamp F. Matrix-assisted ultraviolet laser desorption of non-volatile compounds. Int J Mass Spectrom. 1987;78:53–68.

10. Hillenkamp F, Karas M. Matrix-assisted laser desorption/ionisation, an experience. Int J Mass Spectrom. 2000;200:71–7.

11. Caprioli RM, Farmer TB, Gile J. Molecular imaging of biological samples: localization of peptides and proteins using MALDI-TOF MS. Anal Chem. 1997;69:4751–60.

12. Stoeckli M, Farmer TB, Caprioli RM. Automated mass spectrometry imaging with a matrix-assisted laser desorption ionization time-of-flight instrument. J Am Soc Mass Spectrom. 1999;10:67–71.

13. Dreisewerd K, Schürenberg M, Karas M, Hillenkamp F. Influence of the laser intensity and spot size on the desorption of molecules and ions in matrix-assisted laser desorption/ionization with a uniform beam profile. Int J Mass Spectrom. 1995;141:127–48.

14. Posthumus MA, Kistemaker PG, Meuzelaar HLC, Ten Noever de Brauw MC. Laser desorption-mass spectrometry of polar nonvolatile bio-organic molecules. Anal Chem. 1978; 50:985–91.

15. Zenobi R, Knochenmuss R. Ion formation in MALDI mass spectrometry. Mass Spectom Rev. 1998;17:337–66.

16. Zhigilei LV, Garrison BJ. Molecular dynamics simulation study of the fluence dependence of particle yield and plume composition in laser desorption and ablation of organic solids. Appl Phys Lett. 1999;74:1341–3.

17. Ehring H, Karas M, Hillenkamp F. Role of photoionization and photochemistry in ionization processes of organic molecules and relevance for matrix-assisted laser desorption ionization mass spectrometry. Org Mass Spectrom. 1992;27:472–80.

18. Preston-Schaffter LM, Kinsel GR, Russell DH. Effects of heavy-atom substituents on matrices used for matrix-assisted laser desorption-ionization mass spectrometry. J Am Soc Mass Spectrom. 1994;5:800–6.

19. Knochenmuss R, Zenobi R. MALDI ionization: the role of in-plume processes. Chem Rev. 2003;103:441–52.

20. Breuker K, Knochenmuss R, Zhang J, Stortelder A, Zenobi R. Thermodynamic control of final ion distributions in MALDI: in-plume proton transfer reactions. Int J Mass Spectrom. 2003;226:211–22.

21. Lemaire R, Tabet JC, Ducoroy P, Hendra JB, Salzet M, Fournier I. Solid Ionic matrixes for direct tissue analysis and MALDI imaging. Anal Chem. 2006;78:809–19.

22. Liebl H. Ion microprobe mass analyzer. J Appl Phys. 1967;38:5277–83.

23. Chabala JM, Soni KK, Li J, Gavrilov KL, Levi-Setti R. High-resolution chemical imaging with scanning ion probe SIMS. Int J Mass Spectrom. 1995;143:191–212.

24. Benninghoven A. Die Analyse monomolekularer Festkörperoberflächenschichten mit Hilfe der Sekundärionenemission. Z Physik. 1970;230:403–17.

25. Appelhans AD, Delmore JE. Comparison of polyatomic and atomic primary beams for secondary ion mass spectrometry of organics. Anal Chem. 1989;61:1087–93.

26. Winograd N. The magic of cluster SIMS. Anal Chem. 2005;77:142A–9.

27. Gillen G, Fahey A. Secondary ion mass spectrometry using cluster ion beams. Appl Surf Sci. 2002;203:209–13.

28. Wu KJ, Odom RW. Matrix-enhanced secondary ion mass spectrometry: a method for molecular analysis of solid surfaces. Anal Chem. 1996;68:837–82.

29. Delcorte A, Bour J, Aubriet F, Muller JF, Bertrand P. Sample metallization for performance improvement in desorption/ionization of kilodalton molecules: quantitative evaluation, imaging secondary ion MS, and laser ablation. Anal Chem. 2003;75:6875–85.

30. McDonnell LA, Piersma SR, Altelaar AFM, Mize TH, Luxembourg SL, Verhaert PDEM, van Minnen J, Heeren RMA. Subcellular imaging mass spectrometry of brain tissue. J Mass Spectrom. 2005;40:160–8.

31. Jonkman HT, Michl J, King RN, Andrade JD. Low-temperature secondary positive ion mass spectrometry of neat and argon-diluted organic solids. Anal Chem. 1978;50:2078–82.
32. Ross MM, Colton RJ. Summary abstract: secondary ion mass spectrometry of organic adsorbates on carbon particles and liquid metal surfaces. J Vac Sci Technol A. 1983;1:441–2.
33. Ross MM, Colton RJ. Carbon as a sample substrate in secondary ion mass spectrometry. Anal Chem. 1983;55:150–3.
34. Barber M, Bordoli RS, Sedgwick RD, Tyler AN. J Chem Soc Chem Comm. 1981;325–327.
35. Gillen G, Christiansen JW, Tsong IST, Kimball B, Williams P, Cooks RG. Sputter yields of ammonium chloride and solid glycerol. Rapid Commun Mass Spectrom. 1988;2:67–8.
36. Bennett J, Gillen G. Formation and emission of tetraalkylammonium salt molecular ions sputtered from a gelatin matrix. J Am Soc Mass Spectrom. 1993;4:930–7.
37. Busch KL, Hsu BH, Xie YX, Cooks RG. Matrix effects in secondary ion mass spectrometry. Anal Chem. 1983;55:1157–60.
38. Liu LK, Busch KL, Cooks RG. Matrix-assisted secondary ion mass spectra of biological compounds. Anal Chem. 1981;53:109–13.
39. Wittmaack K, Szymczak W, Hoheisel G, Tuszynski W. Time-of-flight secondary ion mass spectrometry of matrix-diluted oligon- and polypeptides bombarded with slow and fast projectiles: positive and negative matrix and analyte ion yields, background signals, and sample aging. J Am Soc Mass Spectrom. 2000;11:553–63.
40. Delcorte A, Medard N, Bertrand P. Organic secondary ion mass spectrometry: sensitivity enhancement by gold deposition. Anal Chem. 2002;74:4955–68.
41. Delcorte A, Bertrand P. Interest of silver and gold metallization for molecular SIMS and SIMS imaging. Appl Surf Sci. 2004;231–2:250–5.
42. Taban IM, Altelaar AFM, Fuchser J, van der Burgt YEM, McDonnell LA, Baykut G, Heeren RMA. Imaging of peptides in the rat brain using MALDI-FTICR mass spectrometry. J Am Soc Mass Spectrom. 2007;18:145–51.
43. Tempez A, Ugarov M, Egan T, Schultz JA, Novikov A, Della-Negra S, Lebeyec Y, Pautrat M, Caroff M, Smentkowski VS, Wang H-YJ, Jackson SN, Woods AS. Matrix implanted laser desorption ionization (MILDI) combined with ion mobility-mass spectrometry for biosurface analysis. J Proteome Res. 2005;4:540–5.
44. Bunch J, Clench MR, Richards DS. Determination of pharmaceutical compounds in skin by imaging matrix-assisted laser desorption/ionisation mass spectrometry. Rapid Commun Mass Spectrom. 2004;18:3051–60.
45. Jackson SN, Ugarov M, Egan T, Post JD, Langlais D, Schultz JA, Woods AS. MALDI–ion mobility–TOFMS imaging of lipids in rat brain tissue. J Mass Spectrom. 2007;42:1093–8.
46. Müller A, Benninghoven A. Investigation of surface reactions by the static method of secondary ion mass spectrometry: III. The oxidation of vanadium, niobium and tantalum in the monolayer range. Surf Sci. 1973;39:427–36.
47. Plog C, Wiedmann L, Benninghoven A. Empirical formula for the calculation of secondary ion yields from oxidized metal surfaces and metal oxides. Surf Sci. 1977;67:565–80.
48. Standing KG. Timing the flight of biomolecules: a personal perspective. Int J Mass Spectrom. 2000;200:597–610.
49. Wirth A, Thompson G, Gregory SP, editors. In: Benninghoven A, editor. Secondary ion mass spectrometry SIMS VI. New York: Wiley;. 1987. 639 pp.
50. Waugh AR, Kingham DR, Hearn MJ, Briggs DA, editors. In: Benninghoven A, editor. Secondary ion mass spectrometry SIMS VI. New York: Wiley; 1987. 231 pp.
51. Mullock SJ, Reich DF, Dingle T, editors. In: Secondary ion mass spectrometry SIMS VII. New York: Wiley; 1989. 847 pp.
52. Stephens WE, Serin B, Meyerhof WE. A method for measuring effective contact e.m.f. between a metal and a semi-conductor. Phys Rev. 1946;69:42.
53. Schwieters J, Cramer HG, Heller T, Jurgens U, Niehuis E, Zehnpfenning J, Benninghoven A. High mass resolution surface imaging with a time-of-flight secondary ion mass-spectroscopy scanning microprobe. J Vac Sci Technol A. 1991;9:2864–71.

54. Brown RS, Lennon JJ. Mass resolution improvement by incorporation of pulsed ion extraction in a matrix-assisted laser desorption/ionization linear time-of-flight mass spectrometer. Anal Chem. 1998;1995:67.

55. Vestal ML, Juhasz P, Martin SA. Delayed extraction matrix-assisted laser desorption time-of-flight mass spectrometry. Rapid Commun Mass Spectrom. 1995;9:1044.

56. Laiko VV, Dodonov AF. Resolution and spectral-line shapes in the reflecting time-of-flight mass-spectrometer with orthogonally injected ions. Rapid Commun Mass Spectrom. 1994;8: 720–6.

57. Hsieh Y, Casale R, Fukuda E, Chen J, Knemeyer I, Wingate J, Morrison R, Korfmacher W. Matrix-assisted laser desorption/ionization imaging mass spectrometry for direct measurement of clozapine in rat brain tissue. Rapid Commun Mass Spectrom. 2006;20:965–72.

58. Taban IM, Altelaar AFM, van der Burgt YEM, McDonnell LA, Baykut G, Heeren RMA. Imaging of peptides in the rat brain using MALDI-FTICR mass spectrometry. J Am Soc Mass Spectrom. 2007;18:145–51.

59. Kanu AB, Dwivedi P, Tam M, Matz L, Hill Jr HH. Ion mobility-mass spectrometry. J Mass Spectrom. 2008;43:1–22.

60. Gillig KJ, Ruotolo B, Stone EG, Russell DH, Fuhrer K, Gonin M, Schultz AJ. Coupling high-pressure MALDI with ion mobility/orthogonal time-of-flight mass spectrometry. Anal Chem. 2000;72:3965–71.

61. Stauber J, Lemaire R, Wisztorski M, Aït-Menguellet S, Lucot JP, Vinatier D, Desmond A, Deschamps M, Proess G, Rudlof I, Salzet M, Fournier I. New developments in MALDI imaging mass spectrometry for pathological proteomic studies; introduction to a novel concept, the specific MALDI imaging. Mol Cell Proteomics. 2006;5:S247.

62. Lawrence EO, Livingston MS. The production of high speed light ions without the use of high voltages. Phys Rev. 1932;40:19.

63. Comisarow MB, Marshall AG. Fourier transform ion cyclotron resonance spectroscopy. Chem Phys Lett. 1974;25:282–3.

64. Marshall AG, Hendrickson CL, Jackson GS. Fourier transform ion cyclotron resonance mass spectrometry: a primer. Mass Spectrom Rev. 1998;17:1–35.

65. Ledford Jr EB, Rempel DL, Gross ML. Space charge effects in Fourier transform mass spectrometry. Mass calibration. Anal Chem. 1984;56:2744–8.

66. Shi SDH, Drader JJ, Freitas MA, Hendrickson CL, Marshall AG. Comparison and interconversion of the two most common frequency-to-mass calibration functions for Fourier transform ion cyclotron resonance mass spectrometry. Int J Mass Spectrom. 2000;195–196: 591–8.

67. Wisztorski M, Verplanck N, Thomy V, Stauber J, Camart JC, Salzet M, Fournier I. Use of masks in MALDI-MSI: an easy tool for increasing spatial resolution of images by decreasing irradiated area. Indianapolis: American Society of Mass Spectrometry; 2007.

68. Wisztorski M, Croix D, Macagno E, Fournier I, Salzet M. Molecular MALDI imaging: an emerging technology for neuroscience studies. Dev Neurobiol. 2008;68:845–58.

69. Taylor CF, Paton NW, Lilley KS, Binz P-A, Julian RK, Jones AR, Zhu W, Apweiler R, Aebersold R, Deutsch EW, Dunn MJ, Heck AJR, Leitner A, Macht M, Mann M, Martens L, Neubert TA, Patterson SD, Ping P, Seymour SL, Souda P, Tsugita A, Vandekerckhove J, Vondriska TM, Whitelegge JP, Wilkins MR, Xenarios I, Yates JR, Hermjakob H. The minimum information about a proteomics experiment (MIAPE). Nat Biotechnol. 2007;25: 887–93.

70. Orchard S, Hermjakob H. The HUPO proteomics standards initiative—easing communication and minimizing data loss in a changing world. Brief Bioinform. 2008;9:166–73.

71. Sköld K, Svensson M, Norrman M, Sjögren B, Svenningsson P, Andrén PE. The significance of biochemical and molecular sample integrity in brain proteomics and peptidomics: Stathmin 2–20 and peptides as sample quality indicators. Proteomics. 2007;7:4445–56.

72. Theodorsson E, Stenfors C, Mathé AA. Microwave irradiation increases recovery of neuropeptides from brain tissues. Peptides. 1990;11:1191–7.

73. Metz B, Kersten GFA, Hoogerhout P, Brugghe HF, Timmermans HAM, de Jong A, Meiring H, ten Hove J, Hennink WE, Crommelin DJA, Jiskoot W. Identification of formaldehyde-induced modifications in proteins: reactions with model peptides. J Biol Chem. 2004;279: 6235–43.

74. Stauber J, Lemaire R, Franck J, Bonnel D, Croix D, Day R, Wisztorski M, Fournier I, Salzet M. MALDI imaging of formalin-fixed paraffin-embedded tissues: application to model animals of Parkinson disease for biomarker hunting. J Proteome Res. 2008;7:969.

75. Lemaire R, Desmons A, Tabet JC, Day R, Salzet M, Fournier I. Direct analysis and MALDI imaging of formalin-fixed, paraffin-embedded tissue sections. J Proteome Res. 2007;6: 1295–305.

76. Crockett DK, Lin Z, Vaughn CP, Lim MS, Elenitoba-Johnson KSJ. Identification of proteins from formalin-fixed paraffin-embedded cells by LC-MS//MS. Lab Invest. 2005;85:1405–15.

77. Chaurand P, Caprioli RM. Direct profiling and imaging of peptides and proteins from mammalian cells and tissue sections by mass spectrometry. Electrophoresis. 2002;23:3125–35.

78. Stoeckli M, Staab D, Staufenbiel M, Wiederhold KH, Signor L. Molecular imaging of amyloid beta peptides in mouse brain sections using mass spectrometry. Anal Biochem. 2002; 311:33–9.

79. Lemaire R, Wisztorski M, Desmons A, Tabet JC, Salzet M, Fournier I. MALDI-MS direct tissue analysis of proteins: improving signal sensitivity using organic treatments. Anal Chem. 2006;78:7145–53.

80. Altelaar AFM, van Minnen J, Jiménez CR, Heeren RMA, Piersma SR. Direct molecular imaging of *Lymnaea stagnalis* nervous tissue at subcellular spatial resolution by mass spectrometry. Anal Chem. 2005;77:735–41.

81. Lemaire R, Aït-Menguellet S, Stauber J, Marchaudon V, Lucot JP, Collinet P, Farine MO, Vinatier D, Day R, Ducoroy P, Salzet M, Fournier I. Specific MALDI imaging and profiling for biomarker hunting and validation: fragment of the 11S proteasome activator complex, Reg alpha fragment, is a new potential ovary cancer biomarker. J Proteome Res. 2007;6:4127–34.

82. Armin Holle AH, Kayser M, Höhndorf J. Optimizing UV laser focus profiles for improved MALDI performance. J Mass Spectrom. 2006;41:705–16.

83. Lemaire R, Stauber J, Wisztorski M, Van Camp C, Desmons A, Deschamps M, Proess G, Rudlof I, Woods AS, Day R, Salzet M, Fournier I. Tag-mass: specific molecular imaging of transcriptome and proteome by mass spectrometry based on photocleavable tag. J Proteome Res. 2007;6:2057–67.

84. Groseclose MR, Andersson M, Hardesty WM, Caprioli RM. Identification of proteins directly from tissue: in situ tryptic digestions coupled with imaging mass spectrometry. J Mass Spectrom. 2007;42:254–62.

85. Chaurand P, Rahman MA, Hunt T, Mobley JA, Gu G, Latham JC, Caprioli RM, Kasper S. Monitoring mouse prostate development by profiling and imaging mass spectrometry. Mol Cell Proteomics. 2008;7:411–23.

86. Luxembourg SL, McDonnell LA, Duursma M, Guo X, Heeren RMA. Effect of local matrix crystal variations in matrix-assisted ionization techniques for mass spectrometry. Anal Chem. 2003;75:2333–41.

87. Delcorte A. Matrix-enhanced secondary ion mass spectrometry: the alchemist's solution? Appl Surf Sci. 2006;252:6582–7.

88. Wilfried Szymczak KW. Effect of water treatment on analyte and matrix ion yields in matrix-assisted time-of-flight secondary ion mass spectrometry: the case of insulin in and on hydroxycinnamic acid. Rapid Commun Mass Spectrom. 2002;16:2025–33.

89. McArthur SL, Vendettuoli MC, Ratner BD, Castner DG. Methods for generating protein molecular ions in ToF-SIMS. Langmuir. 2004;20:3704–9.

90. Adriaensen L, Vangaever F, Gijbels R. Metal-assisted secondary ion mass spectrometry: influence of Ag and Au deposition on molecular ion yields. Anal Chem. 2004;76:6777–85.

91. Adriaensen L, Vangaever F, Lenaerts J, Gijbels R. Matrix-enhanced secondary ion mass spectrometry: the influence of MALDI matrices on molecular ion yields of thin organic films. Rapid Commun Mass Spectrom. 2005;19:1017–24.

92. Aebersold R, Mann M. Mass spectrometry-based proteomics. Nat Insights. 2003;422: 198–207.
93. Garrison BJ, Winograd N. Ion beam spectroscopy of solids and surfaces. Science. 1982;216: 805–12.
94. Li KW, Smit AB, Geraerts WPM. Structural and functional characterization of neuropeptides involved in the control of male mating behavior of *Lymnaea stagnalis*. Peptides. 1992;13: 633–8.
95. Hanton SD, Clark PAC, Owens KG. Investigations of matrix-assisted laser desorption/ionization sample preparation by time-of-flight secondary ion mass spectrometry. J Am Soc Mass Spectrom. 1999;10:104–11.
96. Stoeckli M, Staab D, Schweitzer A, Gardiner J, Seebach D. Imaging of a [beta]-peptide distribution in whole-body mice sections by MALDI mass spectrometry. J Am Soc Mass Spectrom. 2007;18:1921–4.
97. van Veelen P, Jimenez C, Li K, Wildering W, Geraerts W, Tjaden U, van der Greef J. Direct peptide profiling of single neurons by matrix-assisted laser-desorption ionization mass-spectrometry. Org Mass Spectrom. 1993;28:1542–6.
98. Garden RW, Moroz LL, Moroz TP, Shippy SA, Sweedler JV. Excess salt removal with matrix rinsing: direct peptide profiling of neurons from marine invertebrates using matrix-assisted laser desorption/ionization time-of-flight mass spectrometry. J Mass Spectrom. 1996;31: 1126–30.
99. Redeker V, Toullec J-Y, Vinh J, Rossier J, Soyez D. Combination of peptide profiling by matrix-assisted laser desorption/ionization time-of-flight mass spectrometry and immunodetection on single glands or cells. Anal Chem. 1998;70:1805–11.
100. Stoeckli M, Chaurand P, Caprioli RM. Direct profiling of proteins in biological tissue sections by MALDI mass spectrometry. Anal Chem. 1999;71:5263–70.
101. Garden RW, Sweedler JV. Heterogeneity within MALDI samples as revealed by mass spectrometric imaging. Anal Chem. 2000;72:30–6.
102. Stoeckli M, Chaurand P, Hallahan DE, Caprioli RM. Imaging mass spectrometry: a new technology for the analysis of protein expression in mammalian tissues. Nat Med. 2001;7: 493–6.
103. Rubakhin SS, Greenough WT, Sweedler JV. Spatial profiling with MALDI MS: distribution of neuropeptides within single neurons. Anal Chem. 2003;75:5374–80.
104. Kruse R, Sweedler JV. Spatial profiling invertebrate ganglia using MALDI MS. J Am Soc Mass Spectrom. 2003;14:752–9.
105. Monroe EB, Jurchen JC, Lee J, Rubakhin SS, Sweedler JV. Vitamin E imaging and localization in the neuronal membrane. J Am Chem Soc. 2005;127:12152.
106. Hintersteiner M, Enz A, Frey P, Jaton A-L, Kinzy W, Kneuer R, Neumann U, Rudin M, Staufenbiel M, Stoeckli M, Wiederhold K-H, Gremlich H-U. In vivo detection of amyloid-beta deposits by near-infrared imaging using an oxazine-derivative probe. Nat Biotechnol. 2005;23:577–83.
107. Stauber J, Lemaire R, Wisztorski M, Aït-Menguellet S, Lucot JP, Vinatier D, Desmond A, Deschamps M, Proess G, Rudlof I, Salzet M, Fournier I. New developments in MALDI imaging mass spectrometry for pathological proteomic studies; introduction to a novel concept, the specific MALDI imaging. Mol Cell Proteom. 2006;5:S247.
108. Baluya DL, Garrett TJ, Yost RA. Automated MALDI matrix deposition method with Inkjet printing for imaging mass spectrometry. Anal Chem. 2007;79:6862–7.
109. Hsieh Y, Chen J, Korfmacher WA. Mapping pharmaceuticals in tissues using MALDI imaging mass spectrometry. J Pharmacol Toxicol Meth. 2007;55:193–200.
110. Atkinson SJ, Loadman PM, Sutton C, Patterson LH, Clench MR. Examination of the distribution of the bioreductive drug AQ4N and its active metabolite AQ4 in solid tumours by imaging matrix-assisted laser desorption/ionisation mass spectrometry. Rapid Commun Mass Spectrom. 2007;21:1271–6.
111. Signor L, Varesio E, Staack RF, Starke V, Richter WF, Hopfgartner G. Analysis of erlotinib and its metabolites in rat tissue sections by MALDI quadrupole time-of-flight mass spectrometry. J Mass Spectrom. 2007;42:900–9.

112. Rohner TC, Staab D, Stoeckli M. MALDI mass spectrometric imaging biological tissue sections. Mech Ageing Dev. 2004;126:177–85.
113. Gusev AI, Wilkinson WR, Proctor A, Hercules DM. Direct quantitative analysis of peptides using matrix assisted laser desorption ionization. Fresenius J Anal Chem. 1996;354:455–63.
114. Wilkinson WR, Gusev AI, Proctor A, Houalla M, Hercules DM. Selection of internal standards for quantitative analysis by matrix-assisted laser desorption-ionization (MALDI) time-of-flight mass spectrometry. Anal Bioanal Chem. 1997;357:241–8.
115. Hopfgartner G, Varesio E, Stoeckli M. Matrix-assisted laser desorption/ionization mass spectrometric imaging of complete rat sections using a triple quadrupole linear ion trap. Rapid Commun Mass Spectrom. 2009;23:733–6.
116. Amann JM, Chaurand P, Gonzalez A, Mobley JA, Massion PP, Carbone DP, Caprioli RM. Selective profiling of proteins in lung cancer cells from fine-needle aspirates by matrix-assisted laser desorption ionization time-of-flight mass spectrometry. Clin Cancer Res. 2006;12:5142–50.
117. Burrell MM, Earnshaw CJ, Clench MR. Imaging matrix assisted laser desorption Ionization mass spectrometry: a technique to map plant metabolites within tissues at high spatial resolution. J Exp Bot. 2007;58:757–63.
118. Bunch J, Burrell MM, Clench MR. MALDI imaging to reveal metabolite profiles in potato tubers. Abstract/Comp Biochem Physiol A. 2004;137:147–60.
119. Mullen AK, Clench MR, Crosland S, Sharples KR. Determination of agrochemical compounds in soya plants by imaging matrix-assisted laser desorption/ionization mass spectrometry. Rapid Commun Mass Spectrom. 2005;19:2507–16.
120. Jonathan Stauber, Luke MacAleese J, Franck, Marten Snell, Emmanuelle Claude, basak Kükrer Kaletas, Ingrid van der Wiel, Maxensce Wisztorski, Isabelle Fournier and Ron M.A. Heeren JASMS. On-Tissue Protein Identification and Imaging by MALDI-Ion Mobility Mass Spectrometry. 2010;21:338–47.
121. Robinson S, Warburton K, Seymour M, Clench M, Thomas-Oates J. Localization of water-soluble carbohydrates in wheat stems using imaging matrix-assisted laser desorption/ionization mass spectrometry. New Phytol. 2006;173:428–44.
122. Woods AS, Wang HY, Jackson SN. A snapshot of tissue glycerolipids. Curr Pharm Des. 2007;13:3344–56.
123. Kahn E, Tessier C, Lizard G, Petiet A, Brau F, Clement O, Frouin F, Jourdain JR, Guiraud-Vitaux F, Colas-Linhart N, Siauve N, Cuenod CA, Frija G, Todd-Pokropek A. Distribution of injected MRI contrast agents in mouse livers studied by confocal and SIMS microscopy. Anal Quant Cytol Histol. 2002;24:295–302.
124. Langstrom B, Andren PE, Lindhe O, Svedberg M, Hall H. In vitro imaging techniques in neurodegenerative diseases. Mol Imaging Biol. 2007;9:161–75.
125. Kahn E, Tessier C, Lizard G, Petiet A, Bernengo GC, Coulaud D, Fourré C, Frouin F, Clément O, Jourdain JR, Delain E, Guiraud-Vitaux F, Colas-Linhart N, Siauve N, Cuenod CA, Frija G, Todd-Pokropek A. Analysis of the distribution of MRI contrast agents in the livers of small animals by means of complementary microscopies. Cytometry. 2003;51A:97–106.
126. Acquadro E, Cabella C, Ghiani S, Miragoli L, Bucci EM, Corpillo D. Matrix-assisted laser desorption ionization imaging mass spectrometry detection of a magnetic resonance imaging contrast agent in mouse liver. Anal Chem. 2009;81:2779–84.
127. Shimma S, Sugiura Y, Hayasaka T, Zaima N, Matsumoto M, Setou M. Mass imaging and identification of biomolecules with MALDI-QIT-TOF-based system. Anal Chem. 2008;80:878–85.
128. Stauber J, Kükrer Kaletas B, van der Wiel IM, Snel MF, Claude E, Heeren RMA. Ion mobility imaging mass spectrometry: a new tool for in situ identification proceedings, ASMS Denver. 2008.